

1 Revised manuscript for: *Earth System Dynamics*

2

3 **Groundwater nitrate concentration evolution under climate change**
4 **and agricultural adaptation scenarios: Prince Edward Island,**
5 **Canada**

6

7 Daniel Paradis¹, Harold Vigneault², René Lefebvre², Martine M. Savard¹, Jean-Marc Ballard² and
8 Budong Qian³

9

10 [1] Natural Resources Canada, Geological Survey of Canada, Quebec City, Canada

11 [2] Institut national de la recherche scientifique, Centre Eau Terre Environnement (INRS-ETE),
12 Quebec City, Canada

13 [3] Agriculture and Agri-Food Canada, Eastern Cereal and Oilseed Research Centre, Ottawa,
14 Canada

15 Corresponding author: Daniel Paradis (daniel.paradis@canada.ca)

16 **Abstract**

17 Nitrate (N-NO₃) concentration in groundwater, the sole source of potable water in Prince Edward
18 Island (PEI, Canada), currently exceeds the 10 mg/L (N-NO₃) health threshold for drinking water
19 in 6% of domestic wells. Increasing climatic and socio-economic pressures on PEI agriculture
20 may further deteriorate groundwater quality. This study assesses how groundwater nitrate
21 concentration could evolve due to the forecasted climate change and its related potential changes
22 in agricultural practices. For this purpose, a tridimensional numerical groundwater flow and mass
23 transport model was developed for the aquifer system of the entire Island (5660 km²). A number
24 of different groundwater flow and mass transport simulations were made to evaluate the potential
25 impact of the projected climate change and agricultural adaptation. According to the simulations
26 for year 2050, N-NO₃ concentration would increase due to two main causes: 1) the progressive
27 attainment of steady-state conditions related to present-day nitrogen loadings, and 2) the increase
28 in nitrogen loadings due to changes in agricultural practices provoked by future climatic
29 conditions. The combined effects of equilibration with loadings, climate and agricultural
30 adaptation would lead to a 25 to 32% increase in N-NO₃ concentration over the Island aquifer
31 system. The change in groundwater recharge regime induced by climate change (with current
32 agricultural practices) would only contribute 0 to 6% of that increase for the various climate
33 scenarios. Moreover, simulated trends in groundwater N-NO₃ concentration suggest that an
34 increased number of domestic wells (more than doubling) would exceed the nitrate drinking
35 water criteria. This study underlines the need to develop and apply better agricultural
36 management practices to ensure sustainability of long-term groundwater resources. The
37 simulations also show that observable benefits from positive changes in agricultural practices
38 would be delayed in time due to the slow dynamics of nitrate transport within the aquifer system.

39 1 Introduction

40 Significant increases in groundwater nitrate concentration ($[\text{NO}_3]$) are caused largely by sewage
41 leaks, wastewater treatment without denitrification, improper management of wastewater
42 effluents and overuse of fertilizers and/or animal waste. These nitrate sources are responsible for
43 the contamination of numerous aquifers, especially in those areas where groundwater is
44 replenished directly from the surface over large areas. Nitrate contamination is often associated
45 with anthropogenic activities at ground surface, such as the fertilization of agricultural crops.
46 Once groundwater is contaminated, remediation is difficult, thus the prevention of contamination
47 is the primary strategy used for water quality management (Ghiglieri et al., 2009).

48 Groundwater is the sole source of potable water in the Province of Prince Edward Island (PEI) in
49 eastern Canada, and it plays a dominant role in surface water quality as well. Besides being a
50 concern for drinking water quality, excessive nitrate levels contribute to eutrophication of surface
51 waters, especially in estuarine environments (Somers and Mutch, 1999). Only one watershed
52 among the 50 watersheds delineated in PEI still has groundwater with a mean $[\text{NO}_3]$ within
53 natural background levels (<1 mg/L N- NO_3). Furthermore 6% of supply wells exceed the
54 recommended maximum concentration limit of 10 mg/L (N- NO_3) for drinking water (Health
55 Canada, 2004; Somers, 1998; Somers et al., 1999). Over the past decade, several studies have
56 documented the nitrate problem in PEI groundwater (Somers, 1998; Somers et al., 1999; Young
57 et al., 2002; Savard et al., 2007) and suggested that elevated nitrate levels are often associated
58 with agricultural activities, especially the use of fertilizers for row crop production. In addition,
59 water quality surveys have recorded important increases (more than doubling since 1980) of
60 $[\text{NO}_3]$ in groundwater and surface water in some areas of the province (Somers et al., 1999).

61 According to simulations made with the Global Circulation Model (GCM) for Canada,
62 temperature increases in the order of 2 to 4 °C by 2050 is expected at the country scale
63 (Hengeveld, 2000). Projected changes in annual precipitation over Canada remain within 10% of
64 present levels until 2050, with most of the increases occurring during winter months. Since global
65 warming is expected to change the hydrologic cycle (Gleick, 1986) as well as the agricultural
66 practices (Olesen and Bindi, 2002; McGinn and Shepherd, 2003), it could, in turn, impact
67 groundwater $[\text{NO}_3]$. The overall impact on groundwater $[\text{NO}_3]$ will likely depend on both the
68 magnitude of the change induced by climate change on the hydrologic cycle and how agriculture
69 will adapt to these changes. The combined pressures of climatic change on groundwater recharge

70 and agricultural practices, together with the need to preserve groundwater quality for the
71 residents of PEI illustrate the importance of effective long-term strategies for water management.
72 The aim of this study is then to assess the potential impact of both climate change and modified
73 agricultural practices on future groundwater [NO₃] for the entire PEI (~5 660 km²).

74 Nitrate concentration in groundwater depend on the mass loadings and the amount of water
75 infiltrating the soils down to the water table. In other words, future N-NO₃ concentration can be
76 estimated as the mass of nitrate leached over the volume of recharge per unit area carrying out
77 this mass to the aquifer (groundwater recharge) under projected climatic conditions. Climate
78 change impacts were simulated using different global circulation models (GCMs) and CO₂
79 emission scenarios for the period of 2040-2069, to assess the sensitivity of the climatic variables.
80 The stochastic weather generator AAFC-WG (Hayhoe, 2000) was then used to adjust daily
81 temperature and precipitation of selected large-scale CGM scenarios to the scale of the Island and
82 allow simulations of groundwater recharge over the Island using the hydrologic infiltration model
83 HELP (Schroeder et al., 1994). The physical parameters used by this infiltration model allow an
84 assessment of the impact of changing climatic parameters on the hydrological cycle, which
85 includes groundwater recharge. Moreover, the amount of nitrogen leaching to the aquifer was
86 estimated on the basis of the residual soil nitrogen (RSN) indicator (Yang et al., 2007) under
87 present-day conditions as well as considering agricultural adaptation scenarios in response to the
88 increase of crop heat units, effective growing degree-days and agro-economic trends (De Jong et
89 al., 2008).

90 Studying the impacts of climate change and agricultural management scenarios on groundwater
91 quality also necessitates understanding the aquifer system dynamics. Particularly, flow and
92 transport simulations are needed to assess the nitrate residence time and the aquifer response to
93 changes in practices or climatic conditions. While there have been many studies relating the
94 effect of climate changes on groundwater resources (e.g., Yussof et al., 2002; Allen et al., 2004;
95 Scibek and Allen, 2006; Green et al., 2007a, b; Hsu et al., 2007; Jyrkama and Sykes, 2007;
96 Serrat-Capdevila et al., 2007; Woldeamlak et al., 2007; Holman et al., 2009; Allen et al., 2010;
97 Crosbie et al., 2010; McCallum et al., 2010; Okkonen et al., 2010; Rozell and Wong, 2010; Zhou
98 et al., 2010; Beigi and Tsai, 2015), there are few published studies which attempt to relate climate
99 change to changes in groundwater [NO₃] (e.g., De Jong et al., 2008; Ducharne et al., 2007;
100 Holman et al., 2005a, b; Jackson et al., 2007). In their works, De Jong et al. (2008) and Jackson
101 et al. (2007) estimated mass of nitrogen (N) leaching through the unsaturated zone for different

102 scenarios to relate with $[\text{NO}_3]$ measured in wells. That is, assuming a direct relationship between
103 nitrate leachate and groundwater $[\text{NO}_3]$ regardless of the aquifer system dynamics. While the
104 semi-empirical hydrological model proposed by [Holman et al. \(2005a, b\)](#) to predict $[\text{NO}_3]$ in both
105 surface water and groundwater includes a groundwater store, such model does not simulate
106 spatial and temporal groundwater flow patterns that control nitrate transport in the aquifer
107 system. For instance, [Ducharme et al. \(2007\)](#) demonstrated that modeling of the aquifer system
108 using a physically based groundwater flow model allowed to simulate the inertia of the aquifer
109 system, which has a considerable impact on $[\text{NO}_3]$ measured in wells. In this study, the evolution
110 of groundwater $[\text{NO}_3]$ under a changing climate was modeled using the physically-based
111 groundwater flow and solute transport numerical simulator FEFLOW (Finite Element subsurface
112 FLOW system; [Diersch, 2010](#)) considering the effect of the dual porosity of the fractured porous
113 medium (sandstone), identified by [Jackson et al. \(1990\)](#) as being responsible for the persistence
114 of pesticides in the aquifer system of PEI. In particular, the hydrogeological model developed for
115 the entire Province was based on knowledge gained from the Wilmot watershed ([Jiang and](#)
116 [Somers, 2009](#); [Paradis et al., 2006, 2007](#)), which is representative of most other regions of PEI
117 regarding land use, soils, physiography, geology and hydrogeology. The hydrogeological model
118 was calibrated with historical hydrogeological records of conditions specific to the Island:
119 hydraulic heads, groundwater discharge to river and $[\text{NO}_3]$ measured in both wells and rivers.

120 The novelty of this study is to provide a quantitative comparison of climate change effects and
121 agricultural adaptation impacts on the future evolution of $[\text{NO}_3]$, taking into account potential
122 changes in groundwater recharge and nitrate leached. Also, the general framework developed for
123 the integration of the knowledge related to the aquifer system, climatic parameters and
124 agricultural practices into a comprehensive calibration approach with site-specific records to
125 narrow uncertainty in model parameters, could be applied elsewhere to guide groundwater
126 resource and quality management.

127 **2 Prince Edward Island Study Area**

128 PEI, located in eastern Canada, covers approximately 5 660 km² and is 225 km long by 3 to 65
129 km wide ([Figure 1](#) and [Table 1](#)). Topographic elevation ranges from sea level to 140 m above sea
130 level. PEI is predominantly rural, with 39% of its surface covered by agricultural lands and 45%
131 by forests. Forests mostly cover the eastern and western portions of the Island, whereas

132 agricultural activities are mostly concentrated in the central part. Residential, urban and industrial
133 activities occupy less than 6% of the territory.

134 Figure 1

135 Table 1

136 **2.1 Climate and Hydrology**

137 The climate in the Island is humid continental, with long, fairly cold, winters and warm summers.
138 Data selected from four weather stations geographically distributed across the Island (Figure 1)
139 show relatively similar conditions (Table 2). As an example of the climatic conditions found on
140 the Island, the mean annual precipitation at the Charlottetown weather station is 1173 mm, most
141 of which falls as rain (75%). The mean annual temperature is about 5.3 °C and means for
142 monthly temperature range from -8 °C in January to 18.5 °C in July. The Island can be divided
143 into fifty (50) watersheds comprising 241 sub-watersheds (Figure 1). River basins are typically
144 small, and the main rivers are estuarial over a significant portion of their length. Mean annual
145 streamflow ranges from less than 0.66 to 2.88 m³/s (Table 3).

146 Table 2

147 Table 3

148 **2.2 Geology and Hydrogeological Framework**

149 PEI is a crescent-shaped cuesta of continental red beds, Upper Pennsylvanian to Middle Permian
150 in age, dipping to the northeast at about one to three degrees that consist of conglomerate,
151 sandstone and siltstone in which sandstones are dominant (Van de Poll, 1983). The rock sequence
152 underlying the Island is almost entirely covered by a layer of unconsolidated glacial material
153 from a few centimetres to several meters in thickness (Prest, 1973). These deposits are generally
154 derived from local sedimentary rock and include both unsorted tills and water-worked glacio-
155 fluvial and glacio-marine deposits.

156 With few exceptions, the surficial sediments over PEI do not represent significant aquifers as
157 they are not water saturated, so the sandstone constitutes the main aquifer. Because the geology
158 of the Island is relatively homogeneous, the hydrogeological conceptual model for all PEI is

159 assumed to be similar to the one defined for the Winter River and Wilmot River watersheds
160 where Francis (1989) and Paradis et al. (2006, 2007) carried out extensive hydrogeological
161 characterization. Based on these studies several observations relative to the hydrogeological
162 framework of PEI can be made:

- 163 • The sandstone aquifer comprises a shallow high-flow system overlying a deep low-flow
164 system (Figure 2a). This is based on hydraulic conductivity profiles obtained from field
165 multi-level packer tests in rock aquifer wells that show a rapid decrease of hydraulic
166 conductivity with depth (Figure 2b). This decrease is significant under a depth of 18 to 36 m,
167 according to location. The shallow interval with higher permeability is defined as the high-
168 flow system. Most domestic wells tap potable water in this high-flow system (Mutch, 1998;
169 Rivard et al., 2008).
- 170 • The sandstone aquifer represents a double porosity system with fractures providing
171 groundwater flow paths and the porous matrix providing storage capacity, both for water and
172 solutes, including nitrate. The fractured sandstone is characterized by relatively high
173 hydraulic conductivity, between 1×10^{-6} and 3×10^{-4} m/s (Figure 2b), but it has a low storage
174 capacity (1-3%), as obtained from modelling of baseflow recession curves (Paradis et al.,
175 2006, 2007) and seasonal nitrate sources in groundwater from isotopes (Ballard et al., 2009).
176 In contrast, the matrix has a high porosity of about 17%, but a much lower hydraulic
177 conductivity as measured from laboratory core permeameter tests: mostly between 1×10^{-8}
178 and 5×10^{-7} m/s but as low as 5×10^{-10} m/s for mudstone (Francis, 1989).
- 179 • Comparison between field (Paradis et al., 2006, 2007; Francis, 1989) and laboratory (Francis,
180 1989) hydraulic conductivity measurements suggests that fractures play an important role in
181 the rock aquifer permeability, and the general decrease in hydraulic conductivity with depth
182 is the result of decreasing fracture aperture and frequency. Horizontal bedding of the
183 sandstone forms the main fracture network above 35 m depth (82% of all fractures; Francis,
184 1989). Over a large area, the relative homogeneity of the distribution and interconnection of
185 fractures provides a typical ‘porous media’ response to pumping, especially in the weathered
186 high-flow rock aquifer system (Francis, 1989).
- 187 • Tritium analyses on groundwater samples in the high-flow system indicate the presence of
188 “modern groundwater” younger than 50 years. In the low-flow system, no tritium is observed
189 but Carbon-14 analyses provide groundwater ages between 5 000 and 7 000 years at depths
190 ranging between 50 and 85 m below the water table (Paradis et al., 2006, 2007).

191 • Transient modelling of baseflow recession curves (the groundwater contribution to a river)
192 for the Wilmot River watershed suggests that rivers gain water from the aquifer most of the
193 year (Jiang and Somers, 2009) and there is a strong interaction between the high-flow system
194 and the rivers (Paradis et al., 2007). This is also supported by seasonal sampling of nitrate
195 carried out over a period of two years in domestic wells and in the Wilmot River that shows
196 similar average [NO₃] as well as water and nitrate isotope properties (Savard et al., 2007;
197 Savard et al., 2010).

198 In summary, it is inferred from the development of the conceptual hydrogeological model that
199 groundwater flow and nitrate transport predominantly occur in the high-flow system (Figure 2c).
200 The shallow high-flow system essentially follows the ground topography and is hydraulically
201 connected to rivers. Nitrate transported to the aquifer by infiltration of precipitation will first
202 reach the shallow high-flow system and then eventually reach rivers mainly through fractures in
203 weathered and fractured sandstone, which are fairly more permeable than the sandstone matrix
204 itself. Nitrate transport rate through the aquifer system could however be reduced as matrix
205 diffusion occurs due to the contrast in [NO₃] between fractures and matrices. The high porosity of
206 the sandstone matrix makes it an important repository for nitrate which could store or release
207 nitrate, depending on geochemical conditions in the adjacent fracture network. Finally, it is also
208 likely that a proportion of the nitrate transported in the high-flow system has also reached the
209 underlying low-flow system. Considering the reduced groundwater flow and the mostly old
210 groundwater ages encountered in the low-flow system, the nitrate that may be present in the low-
211 flow system may not have reached rivers yet. Note that in the case of the entire PEI, oxidizing
212 aquifer conditions usually prevail in the sandstone aquifer and it was assumed that denitrification
213 processes are negligible within the aquifer. Moreover, no natural geological sources of nitrate are
214 expected to be present throughout the Island. The aquifer [NO₃] would then be controlled by
215 water infiltration and nitrate leaching from the soil.

216 Figure 2

217 3 Study Methodology

218 Figure 3 presents the general workflow followed to model the evolution of [NO₃] in groundwater
219 of the PEI aquifer system, which is briefly described below with further details provided in the
220 following sections:

- 221 • Climate change can itself be predicted on the basis of meteorological models with a large
222 degree of uncertainty. Therefore, different climate change scenarios have to be considered in
223 order to represent the potential range of impacts related to predicted temperature and
224 precipitation. In this study, four climate scenarios were selected to provide future daily
225 weather conditions for the period 2040-2069. These scenarios are based on different global
226 circulation models (GCMs) and CO₂ emission scenarios for the period 2040-2069.
- 227 • The daily temperatures and precipitations of the four selected large-scale CGMs were
228 downscaled using historical meteorological records of existing weather stations using the
229 stochastic weather generator AAFC-WG (Hayhoe, 2000) in order to provide more realistic
230 climate conditions of the Island.
- 231 • Groundwater recharge was obtained from the HELP infiltration model (Schroeder, 1994),
232 which uses daily climate conditions and soil properties as input. As done by Croteau et al.
233 (2010), recharge obtained from HELP was calibrated on the basis of present-day climate
234 conditions, so that future recharge could be estimated using the four climate scenarios.
- 235 • Nitrate leaching to the aquifer system was estimated under present-day conditions and
236 agricultural adaptation scenarios. This mass of nitrate leachate is determined on the basis of
237 the residual soil nitrogen (RSN) indicator (Yang et al., 2007).
- 238 • Using present-day nitrate mass and groundwater recharge, a three-dimensional numerical
239 model of groundwater flow and nitrate transport was developed and calibrated to represent
240 the specific hydrogeological conditions of PEI using FEFLOW (Diersch, 2004). This model
241 was then used to simulate the future evolution of [NO₃] under different climate change and
242 agricultural adaptation scenarios that implied potential changes in groundwater recharge and
243 nitrate leachate.

244 Figure 3

245 3.1 Climate Change Scenarios and Climate Data Downscaling

246 The Intergovernmental Panel on Climate Change Special Report on Emission Scenarios
247 (Nakicenovic and Swart, 2000) provides 40 different scenarios, which are all deemed ‘equally
248 likely’, but the A2 and B2 scenarios are widely adopted in climate change experiments and
249 impact studies (IPCC, 2001). The A2 scenario envisions a population growth to 15 billion by
250 year 2100 with rather slow economic growth and development. Consequently, the projected

251 equivalent CO₂ concentration rises from 476 ppm in 1990 to 1320 ppm in 2100. The B2 scenario
252 envisions slower population growth (10.4 billion by 2100) with a more rapidly evolving
253 economy, but with more emphasis on environmental protection. It therefore produces lower
254 emissions (CO₂ concentration of 915 ppm by 2100) and less warming than scenario A2. The A2
255 and B2 scenarios were simulated using two different GCMs, which are the CGCM2 (Flato and
256 Boer, 2001) developed at the Canadian Centre for Climate Modelling and Analysis, and HadCM3
257 (Gordon et al., 2000) developed at the Hadley Centre for Climate Prediction and Research of the
258 UK Meteorological Office. Daily outputs of maximum and minimum air temperature, and total
259 precipitation were obtained electronically from the Canadian Centre for Climate Modelling and
260 Analysis and the Hadley Centre through the Climate Impacts LINK project (Viner, 1996) for the
261 four climate change scenarios labelled hereafter: CGCM2-A2, CGCM2-B2, HadCM3-A2 and
262 HadCM3-B2.

263 The AAFC-WG (Hayhoe, 2000) was used to generate synthetic continuous daily weather records
264 for the historical period (1971-2000) and for two (2040-2069) climate scenarios using different
265 GCMs (Figure 3). The time period 2014-2069 is approximately corresponding to a doubling of
266 atmospheric CO₂ concentration (Qian et al., 2010). The AAFC-WG is a stochastic weather
267 generator that was developed for and evaluated in diverse Canadian climates (Qian et al., 2004).
268 To obtain future climate data, daily outputs from the four climate change scenarios (CGCM2-A2,
269 CGCM2-B2, HadCM3-A2 and HadCM3-B2) were downscaled with observed historical climate
270 data from existing weather stations. A total of eleven weather stations were selected, covering
271 PEI fairly evenly and having the best available historical weather data for 1971-2000 (Figure 1).
272 Observed historical weather data, including daily maximum and minimum air temperatures and
273 daily precipitation, were provided by Environment Canada through their web site, and first used
274 to calibrate an AAFC-WG model for each weather station. The parameters for the various
275 statistical models used by the AAFC-WG were indeed estimated from historical observations
276 independently for each station. Note that historical climate from synthetic weather data generated
277 by AAFC-WG is generally not significantly different from observations (Qian and De Jong,
278 2007; Qian et al., 2011).

279 **3.2 Groundwater Recharge**

280 Groundwater recharge simulations serving as input for the FEFLOW model was carried out with
281 the physically based hydrologic model HELP (Schroeder et al., 1994) (Figure 3). The model is

282 quasi two-dimensional and the natural water balance components simulated include precipitation,
283 interception of rainwater by leaves, evaporation by leaves, surface runoff, evaporation from soil,
284 plant transpiration, snow accumulation and melting, and percolation of water through the soil
285 profile. The advantage of using such a model is that temperature and precipitation resulting from
286 climate scenarios may be directly used in the model to predict future groundwater recharge, once
287 the model has been calibrated based on present-day data (e.g., [Jyrkama et al., 2002](#); [Allen et al.,](#)
288 [2004](#); [Croteau et al., 2010](#); [Rivard et al., 2014](#)).

289 The spatial estimation of groundwater recharge over PEI was obtained using 500x500 m cells
290 (total of 21 168). For each cell, model parameters were retrieved and analyzed with geographical
291 information software and a database management system. The HELP parameters used are
292 summarized below.

- 293 • Soil profile: The soil profile is the vertical combination of natural soil and geological
294 materials that compose the vadose and saturated zones. The surface soil information was
295 assembled from various regional soil surveys conducted on the Island ([Canadian Soil](#)
296 [Information System, 2000](#)). There were a total of 953 unique soil types identified on PEI that
297 were regrouped into 6 distinct soil classes according to the dominant soil texture (A-Sand or
298 coarser ; B-Loamy sand or gravelly ; C-Sandy loam (<8% clay); D-Fine sandy loam or
299 very fine sandy loam ; E-Loam or silt loam ; and F-Sandy clay loam or clay loam). A typical
300 soil profile consisting of three layers was used to their representation. The top layer is 0.5 m
301 thick and consists of one of the 6-soil class; layer 2 is 1-17 m thick and consists of
302 unconsolidated glacial material; and bottom layer is 10 m thick and consists of weathered
303 sandstone (high-flow system).
- 304 • Initial moisture content: The initial water content of each soil profile layers was computed by
305 the model as steady state values. HELP indeed assigned values for the initial water moisture
306 storage of layers and simulates a one-year period. These values were then used as initial
307 values for the simulations. A sensitivity analysis of initial water content reveals that this
308 parameter does not affect significantly groundwater recharge estimates as steady state
309 conditions can be assumed over the long simulation period.
- 310 • Surface runoff: Surface runoff (also known as overland flow) is the flow of water that occurs
311 when excess rainfall or snowmelt flows over the soil surface. Surface runoff was estimated
312 using modified Soil Conservation Service (SCS) curve-number method ([USDA, 1986](#)), as

313 proposed by [Monfet \(1979\)](#). The modified method allows a more reliable estimation of
314 surface runoff in watersheds with short concentration time and for precipitation patterns
315 found in eastern Canada. The modified SCS method allows estimation of surface runoff to a
316 river following a rainfall or snowmelt event using soil characteristics, land use, type of
317 vegetation, soil humidity, and surface slope. Digital land use and land cover data were
318 obtained from Landsat-7 images ([CanImage, 2001](#)).

- 319 • Solar radiation: The required daily values of precipitation, mean air temperature, and solar
320 radiation were calculated. Precipitation and temperature were obtained from downscaled
321 climate scenarios, while solar radiation data were generated using the weather generator
322 provided by HELP. Solar radiation is computed according to precipitation (whether the day
323 is wet or dry) and latitude.
- 324 • Evapotranspiration: The multi-layer procedure for calculating evaporation values from snow,
325 soil, and leaves, as well as transpiration based on type of vegetation used the evaporative
326 zone depth, maximum leaf-area index, growing season start and end day, average wind
327 speed, and relative humidity. These parameters were evaluated from existing land cover,
328 agricultural and climatic data.

329 Groundwater recharge values simulated from HELP were calibrated against baseflow values
330 estimated using the method of hydrograph separation with streamflow records ([Furey and Gupta;](#)
331 [2001](#)) to narrow uncertainty in the input parameters of HELP (e.g., [Croteau et al., 2010](#)).
332 Baseflow is the groundwater contribution to river discharge (streamflow) and it is often used as
333 an approximation of groundwater recharge when underflow (groundwater flow beneath and by-
334 passing a river), evapotranspiration from riparian vegetation, and other losses of groundwater
335 from the watershed are minimal ([Risser et al., 2005](#)). Hydrograph separation methods estimate
336 the part of the streamflow hydrograph attributed to baseflow using semi-empirical filter
337 techniques. The calibration was done with the historical records of temperature and precipitation
338 (1971-2000) for three gauged streamflow stations with the most comprehensive time series
339 (Morell, Wilmot and Winter, [Figure 1](#) for location). For each watershed, groundwater recharge
340 with HELP was estimated by summing all individual 1D soil profiles included in the watershed
341 assuming that water reaching the aquifer for each soil profile contributes to the streamflow within
342 the year. The most relevant parameters to calibrate were the evaporative zone depth and the heat
343 insulation of the snow cover. The trend in groundwater recharge simulated with HELP is
344 comparable to baseflow estimated with the [Furey and Gupta \(2001\)](#) method ([Table 4](#)), with a

345 correlation coefficient of 0.64 and no significant bias (relative error close to 0) in the annual
346 values. The error in the simulated values is 19% as expressed by the RMS error.

347 Table 4

348 3.3 Mass of Nitrogen Available for Leaching and Agricultural Adaptation Scenario

349 The mass of nitrate available for transfer to groundwater was estimated with the residual soil
350 nitrogen (RSN) indicator (Drury et al., 2007; Figure 3). The RSN indicator estimates the quantity
351 of inorganic soil N at the time of harvest, at the Soil Landscape of Canada (SLC) polygon level
352 (Soil Landscapes of Canada Working Group, 2006). The RSN indicator is the difference between
353 N inputs from chemical fertilizer N, manure, biological N fixation by leguminous crops, and
354 atmospheric deposition and outputs in the form of N in the harvested portion of the crops and
355 pasture, and gaseous (N₂ and N₂O) losses to the atmosphere via denitrification. The total
356 chemical fertilizer N is based on fertilizer recommendation applied to crops adjusted to the total
357 manure N available for crops and improved pasture. The amount of available inorganic N from
358 manure applied to crops and pasture take into consideration losses from storage and handling. It
359 is estimated that 15% of manure N is lost during storage and handling (Burton and Beauchamp,
360 1986), 35% is added to the soil as organic N (Ontario Ministry of Agriculture and Food, 2003),
361 and consequently 50% of N originally present in manure is inorganic N which would be available
362 to crops during the year of application. Of this available N, 1.25% is lost as N₂O emissions, and
363 an equal portion is assumed to be lost through N₂ production. Although soil mineralization and
364 immobilization also occur on a seasonal basis, it is assumed that soils are in a steady-state
365 situation, with no net change in soil organic N from one year to the next.

366 The main inputs of the RSN model consist of acreages for all major agricultural crops and their
367 associated crop yields, as well as the type and number of livestock. These data are collected every
368 five years through the census made by Agriculture and Agri-Food Canada and are allocated to
369 SLC polygons based on the methodology described by Huffman et al. (2006). The RSN model
370 was run for all five-census years (1981, 1986, 1991, 1996 and 2001) and the output was averaged
371 to obtain a 'historical' RSN value for each of the 23 SLC polygons covering PEI (De Jong et al.,
372 2008). The RSN values at the SLC polygon level could not be validated because independent
373 data sets are not available at that scale. However, Yang et al. (2007) compared the total adjusted
374 chemical fertilizer N recommendation (fertilizer recommendation minus available manure) with

375 the total amount of N fertilizer sold in PEI. For the five census, the average ratio between the
376 adjusted fertilizer recommended rates and the amount of N fertilizer sales is 1.0 (between 1.35 to
377 0.82) indicating that fertilizer recommendations are generally well followed in the province.

378 Many different agricultural adaptation scenarios can be devised, either with increased or
379 decreased production intensity as compared to the present level. For the purpose of our study, a
380 «worst case» scenario was selected because none of the adaptation scenarios is verifiable. Based
381 on consensus expert opinion of Agriculture and Agri-Food Canada at the Research and Policy
382 Branch, it was assumed that agricultural production in PEI would intensify over the next 50
383 years. Hence, relative to the 2001 census provincial totals, the following sequential agricultural
384 land use scenario was developed for the 2040-2069 period (De Jong et al., 2008):

- 385 • The area of alfalfa, improved pasture, tame hay and other grain cereals reduces by 40, 30, 30
386 and 15%, respectively (total ‘freed-up’ area: 29 794 ha);
- 387 • The berries and vegetable area increases by 100% (remaining ‘freed-up’ area: 25 179 ha);
- 388 • Of the remaining ‘freed-up’ area, 20, 40 and 40% is allocated to potatoes, grain corn and
389 soybeans, respectively;
- 390 • Buffer strips, a legislative requirement, reduce the increased total area of potatoes by 5%,
391 with this area going into the ‘other land’ category;
- 392 • For SLCs 538001, 537002 and 537003, the total area of potatoes decreases by 6%, because
393 these SLCs contain fields with steep slopes, and the ‘freed-up’ area is allocated equally to
394 tame hay and spring wheat;
- 395 • As a consequence of the decrease in perennial forages, the number of cattle decreases by
396 10%; and
- 397 • The number of poultry and pigs increases by 30%.

398 To calculate RSN for this agricultural adaptation scenario, the 1996 crop yields and N
399 fertilization recommendations of Ontario were used because crop heat units and effective
400 growing degree-days for this year were reported to be similar than those reported for the 2040-
401 2069 period in PEI (Bootsma et al., 2001). Thus, the agricultural adaptation scenario depends on
402 land use, crop yield and N fertilization recommendation changes induced by climate change. As
403 done by De Jong et al. (2008), the RSN model was then run with this scenario to obtain 23
404 projected RSN values one for each polygon. The N mass was applied on the SLC polygons
405 because RSN values are estimated over these entire polygons. RSN units are provided in kg of N

406 per hectare of farmland area but farmlands are not defined within the SLC polygon. To provides
407 conservative scenarios, it was assumed that the total RSN was nitrified and leached to the aquifer
408 within the year. Moreover, to be compatible with the FEFLOW model, the transformed mass of
409 N applied at the surface of the model was estimated by multiplying the RSN values by the ratio
410 of farmland area over SLC polygon area. This operation maintains the total mass of nitrate over
411 the SLC polygon but reduces the applied rate.

412 **3.4 Numerical Groundwater Flow and Nitrate Transport Model**

413 The physically based FEFLOW model used to simulate groundwater flow and nitrate transport
414 was divided into eight layers (4 layers for each of the two flow systems). The base of the model is
415 deep at 800 m below water table to include the different flow patterns that can develop within the
416 PEI aquifer system (e.g., Tóth, 1963). The flow in the vadose zone was neglected due to the short
417 lag-time response (few days) between precipitations and water table fluctuations. Boundary
418 conditions include constant heads around the Island in the first layer, and no flow boundaries in
419 the underlying layers to simulate the flow along the saline front around the Island. Constant heads
420 were also applied to rivers on the first layer to represent the hydraulic connection between rivers
421 and the high-flow system. Note that non-pumping conditions were considered for the calibration
422 and future scenarios, as most of the Island is supplied by individual domestic wells sparsely
423 spread over the Island (approximately 145 000 inhabitants in 2014, over 5 660 km²). The impact
424 of pumping wells on the water table is thus expected to be low (<2 mm/y based on a daily
425 individual consumption of 200 L), except in few localized areas where potable water is supplied
426 by production wells (e.g., Charlottetown). Irrigation water for agriculture and associated return
427 flow were not considered either because rainfall generally supplies the needed water demand for
428 crops irrigation. The resulting three-dimensional grid contains 4 896 246 6-node prismatic
429 triangular elements with an average element area of 0.0925 km² (with triangle edges of
430 approximately 430 m).

431 The calibration of the FEFLOW model, which is an important step to narrow uncertainty in
432 historical and future groundwater [NO₃], was carried out sequentially with three independent data
433 sets: (1) hydraulic heads measured in domestic wells; (2) baseflow-recession curves for the main
434 rivers and; (3) groundwater [NO₃] recorded in domestic wells.

435 3.4.1 Hydraulic Heads Calibration

436 The calibration of the FEFLOW model was first carried out under steady-state conditions with
437 hydraulic head values measured at the time of drilling in more than 700 wells. These wells are
438 domestic water wells, of varying depth, which generally end in the shallow high-flow system.
439 Hydraulic heads were used to adjust the horizontal and vertical hydraulic conductivities within
440 the reported range of values (Table 5) while keeping calibrated groundwater recharge values from
441 the HELP model unaltered. The mean annual groundwater recharge for the 1971-2001 period was
442 used. Using a time-averaged recharge value per model cell to represent present-day groundwater
443 recharge conditions is justified by the facts that: (1) no significant changing trend is observed in
444 water table elevation at available long-term monitoring well hydrographs over the Island (Rivard
445 et al., 2009); and (2) measured head data were collected over a considerable period of time (>40
446 years). A comparison of the observed and predicted hydraulic heads indicates a similar trend with
447 a relatively high correlation coefficient of 88%, but show a fair amount of scatter and simulated
448 heads slightly underestimated (Table 4). This is consistent with the fact that the observed head
449 data were measured over several decades and likely reflect transient intra and inter-annual head
450 variations, which results in large uncertainty in mean head values, which is what the numerical
451 groundwater flow model represents.

452 Table 5

453 3.4.2 Baseflow-Recession Calibration

454 Once an acceptable match was obtained under steady-state conditions, the resulting model was
455 used to simulate transient baseflow under recession conditions for the main rivers (Morell,
456 Wilmot, Winter) to estimate specific yield (Table 5). With this procedure, groundwater recharge
457 for the model is set to zero and daily discharge through the river nodes are compared to specific
458 baseflow-recession events extracted from streamflow records. Baseflow-recession events for PEI
459 occur generally at the end of summer during long periods of time without rainfall, when rivers are
460 solely sustained by groundwater. The rate of decline of baseflow-recession curves is sensitive to a
461 specific yield value, which controls the amount of water that can drain from the aquifer to the
462 connected rivers (Mendoza et al. 2003; Sánchez-Murillo et al., 2015). A lower specific yield
463 value is thus associated to a faster drainage of the aquifer. This dynamic is linked with
464 groundwater and nitrate residence time that have a direct impact on the capabilities of the

465 numerical model to predict meaningful groundwater [NO₃]. The modelling of baseflow-recession
466 events shows the best adjustment for a specific yield value of 1% (Table 4), which is attributed to
467 the fractures in the sandstone aquifer. Note that recession curves are mostly sensitive to the high-
468 flow layers, and specific yield values for underlying layers were progressively lowered to
469 represent the decreasing number of fractures with depth (Table 5).

470 3.4.3 Nitrate Concentrations Calibration

471 After calibration of the groundwater recharge with HELP and the aquifer system dynamics with
472 FEFLOW through head and baseflow-recession data, the historical mass of N leaching to the
473 aquifer was adjusted to match present-day (2000-2005) [NO₃] measured in more than 17,000
474 domestic wells. In PEI, intensive agriculture began around 1965 with the introduction of
475 chemical fertilizers and steadily increased since that time. The model of Paradis et al. (2006,
476 2007) for the Wilmot River watershed has illustrated the considerable time lag between increased
477 leaching of nitrate and the build up of groundwater [NO₃] corresponding to this increased input.
478 This lag time is due to both the large capability of the PEI aquifer system to accumulate nitrate
479 because of the large porosity of the sandstone, and the typically long residence time of
480 groundwater from its recharge to its outflow in rivers. The maximum residence time of the high-
481 flow and the shallow low-flow systems before discharge to the Wilmot River watershed was up
482 to 20 and 10 000 years, respectively. It can be assumed that a similar situation exists over the
483 entire PEI aquifer system and that groundwater [NO₃] is presently not in steady state equilibrium
484 with the nitrate leachate that have historically prevailed in watersheds throughout PEI.
485 Consequently, the numerical model needs to be run under transient conditions with the historical
486 record of the mass of nitrate reaching the aquifer to ensure realistic predictions of groundwater
487 [NO₃]. Because RSN values were only estimated based on the 5 census years (1981, 1986, 1991,
488 1996, 2001), no RSN estimate is available prior to 1981. Thus, for the onset of intensive
489 agriculture in PEI from 1965 to 1981, an average mass of nitrate representative for this period
490 was adjusted to match observed present-day [NO₃]. The estimates of mass of nitrate leaching to
491 the aquifer based on the last 5 census years were not modified during the calibration process and
492 it was assumed that all available RSN is transferred to the aquifer within the year of application.

493 As previously demonstrated by Savard et al. (2007), no significant denitrification occurs in the
494 PEI aquifer system, and then only advective-dispersive transport was considered. Groundwater
495 flow and nitrate transport were then run under steady-state and transient conditions, respectively,

496 using hydraulic parameters summarized in Table 5. Total porosity needed for the transport
497 simulations were based on average laboratory values (Francis, 1989), whereas the effective
498 diffusion coefficient, and longitudinal and transverse dispersivities were $1 \times 10^{-9} \text{ m}^2/\text{s}$, 5 m and 0.5
499 m, respectively, considering typical groundwater flow path lengths (Gelhar et al., 1992).

500 As reported in Table 4, the average $[\text{NO}_3]$ measured in wells generally agrees with the simulated
501 concentration for the SLC polygons for which RSN values are available. Simulated concentration
502 is the average $[\text{NO}_3]$ for the first four layers representing the high-flow system within which most
503 domestic wells are installed. However, the simulated concentration slightly underestimates
504 measurements (approximately 0.5 mg/L lower), as expected from the procedure of nitrate mass
505 application at the surface of the model previously discussed. Based on the RMS value, the error
506 in groundwater $[\text{NO}_3]$ predicted by the FEFLOW model is 30%.

507 **4 Results of Modelling**

508 On the basis of the previous calibration results, it is assumed that the FEFLOW model provides a
509 good representation of groundwater flow conditions and nitrate transport in the PEI aquifer
510 system as well as of present-day $[\text{NO}_3]$ in drinking water. For the purposes of this study, and
511 knowing the uncertainty about groundwater recharge, hydraulic conductivity, specific yield,
512 porosity and nitrate mass, consideration will thus be given to the relative changes of future
513 scenarios with respect to the calibrated FEFLOW model.

514 **4.1 Future Climate Scenarios**

515 The generated future climate scenarios show considerable warming from both GCMs (Table 6),
516 although CGCM2 projected much greater warming than HadCM3 for the Charlottetown weather
517 station (Figure 1). Also, minimum temperature increases more markedly than maximum
518 temperature, and warming under scenario A2 is more noticeable than under B2, as expected from
519 higher CO_2 emissions. While warming is expected throughout the entire year (July and January)
520 for all scenarios, changes in precipitation appear uncertain, with total monthly precipitation and
521 number of days with precipitation increasing or decreasing according to a specific scenario or
522 season. Indeed, CGCM2 projects a slight decrease in precipitation for January with the opposite
523 for HadCM3, even though the number of days with precipitation decreases in January for all
524 scenarios. However, the projected July precipitation for 2040-2069 shows an increase or no
525 change relative to the 1971-2000 averages for all four scenarios.

526 Scenario CGCM2-A2 shows a decrease in precipitation intensity during July (summer), as the
527 number of days with precipitation increases and total precipitation remains unchanged. This can
528 thus have an impact on surface runoff because a decrease in precipitation intensity results in less
529 excess water to runoff during rainfall events. The scenario HadCM3-A2 shows on the contrary an
530 increase in precipitation intensity for July. For January (winter), the surface runoff dynamics is
531 more complex as snowpack thawing and form of precipitation (snow vs rain) should be taken into
532 account as previously done with the HELP model.

533 Table 6

534 **4.2 Hydrologic Cycle Components and Groundwater Recharge**

535 Simulation results for the historic period (1970-2001) show that almost 50% (583 mm) of the
536 annual precipitation is returned to the atmosphere by evapotranspiration (Table 7). Another 19%
537 (221 mm) is flowing to the rivers by surface runoff, and 31% (369 mm) infiltrates the soil down
538 to the sandstone aquifer as groundwater recharge. Moreover, groundwater recharge over the
539 Island varies from 0 mm/yr in wetland areas, to 704 mm/yr over coarse sand soil (Figure 4). The
540 standard-deviation for groundwater recharge values is 50 mm/yr, in accordance with the
541 homogeneity observed at the Island scale for climate as well as for the soil and geology.

542 For the 2040-2069 period, evapotranspiration values increase for all climate scenarios, as
543 expected from the increase in temperature for the same period (Table 7). However, the variation
544 in evapotranspiration is less marked than the variation in temperature. For surface runoff, values
545 are predicted to be unchanged or decreased, with large variations ranging from 0 to 66 mm (Table
546 7). Those variations between scenarios are mainly related to the total precipitation available,
547 evapotranspiration, decrease in precipitation intensity and snowpack dynamics as previously
548 discussed. Total precipitation and groundwater recharge variations between scenarios follow
549 similar patterns with increased values for the A2 scenarios (CGCM2 and HadCM3) and
550 decreased values for the B2 scenarios with respect to the historic period (Table 7). In general, a
551 decrease in groundwater recharge is expected for the 2040-2069 period (between 2.1 to 12.4%);
552 only the CGCM2-B2 scenario leads to an increase in recharge of 6.7%.

553 Table 7

554 Figure 4

555 4.3 Residual Soil Nitrogen

556 The components of the N balance were averaged over the 23 SLC polygons in PEI (Table 8). The
557 total amount of N input from fertilizer, manure, leguminous crops and atmospheric deposition is
558 102.3 kg N/ha/yr. The outputs consist in N removed by cropping and gaseous losses, which total
559 71.5 kg N/ha/yr. The province-wide average RSN is therefore 30.8 kg N/ha/yr. The spatial
560 variability of historical RSN values ranges from less than 25 kg N/ha/yr to approximately 40 kg
561 N/ha/yr according to the local agricultural management practices (Figure 5a).

562 With the agricultural adaptation scenario, N inputs from fertilizer were predicted to increase by
563 8.4 kg N/ha/yr relative to historical inputs (Table 8). The other inputs from manure, fixation and
564 deposition remained relatively constant. N removal by crop uptake increases by 3.1 kg N/ha/yr,
565 and consequently residual soil N at the end of the growing season increases significantly from
566 30.8 kg N/ha/yr under historical management, to 35.7 kg N/ha/yr with the simulated adaptation
567 scenario (16% increase). The spatial variability of RSN under the adaptation scenario ranges
568 from 28.3 kg N/ha/yr to 46.1 kg N/ha/yr (Figure 5b). The increase in RSN relative to historical
569 data ranges from 10 to 23%.

570 Table 8

571 Figure 5

572 4.4 Nitrate Concentration Evolution Simulations

573 To assess the potential impact of climate change and agriculture adaptation in the future, nine
574 groundwater flow and mass transport simulation scenarios were defined:

- 575 • Scenario 1 (Figure 6b): This is the baseline scenario, which uses the mean historical
576 groundwater recharge (steady-state flow) and the present-day agricultural practices (steady-
577 state transport with RSN values from the 2001 census) from 2001 until 2069. This scenario is
578 used to assess when aquifer concentrations are reaching steady-state conditions using
579 present-day nitrate mass (equilibrium between nitrate inputs and outputs from the aquifer
580 system).
- 581 • Scenarios 2 to 5 (Figures 7a-d): These scenarios use the present-day agricultural practices
582 (steady-state transport) in the SLC polygons but their groundwater recharge is based on the

583 values obtained from the four climate scenarios (transient flow). The mass of nitrate applied
584 over the watershed is kept constant for the 23 SLC polygons from 2001 until 2069. This
585 mass represents the mean RSN value from the 5 past censuses (1981, 1986, 1991, 1996 and
586 2001). These scenarios combine the impact of aquifer system equilibrium and groundwater
587 recharge change related climate changes on $[\text{NO}_3]$.

588 • Scenarios 6 to 9 (Figures 8a-d): These simulations use the RSN values modelled for the
589 2040-2069 period (transient transport) with the four climate scenarios along with the
590 groundwater recharge based on the values obtained from these climate scenarios (transient
591 flow). These scenarios combine the impact of $[\text{NO}_3]$ equilibrium, groundwater recharge
592 change and agricultural adaptation (land use and climate changes).

593 For the modelling purposes of this study, the gap between the last year of the calibration period
594 (2001) and the beginning of the scenarios (2040) was then filled with gradual changes in
595 groundwater recharge and RSN values to provide meaningful $[\text{NO}_3]$ in the future. A linear
596 interpolation between values established for 2001 and 2040 was thus applied.

597 Figure 6a presents map of the average $[\text{NO}_3]$ per watershed for the present-day (2001) conditions
598 obtained from the calibrated FEFLOW model. For comparison purposes, modelled groundwater
599 $[\text{NO}_3]$ were divided into four classes: background (<1 mg/L), low (1-3 mg/L), medium (3-5
600 mg/L) and high (>5 mg/L). These classes are used to emphasize that the model is more indicative
601 of relative spatio-temporal changes in groundwater $[\text{NO}_3]$ rather than absolute concentration
602 values. This map shows that the most impacted watersheds are in the center of the Island where
603 most agricultural activities are taking place. Histograms of the number of watersheds in each
604 class reveal that 42% of the watersheds are in the medium (17) or high (4) $[\text{NO}_3]$ classes (Figure
605 6a; Table S1). This observation reflects the critical situation PEI is in regarding groundwater
606 quality related to nitrate contamination.

607 Note that for simplicity results are presented for 2050 (middle of the period 2014-2069).
608 Compared to the present-day situation (Figure 6a), the average increases in $[\text{NO}_3]$ for the 2050
609 baseline scenario (scenario 1; Figure 6b) is 11% for the Island (Table S1). This increase reflects
610 steady-state in groundwater concentration due to gradual loading of nitrate using present-day
611 concentration. Under the 2050 baseline scenario, the average nitrate content of several
612 watersheds moves in a higher concentration class, 50% to the medium (17) and high (8) classes.
613 The 2050 results show no more watershed at the background level (Figure 6b; Table S1).

614 Moreover, in the Western part of the Island, several watersheds are predicted to reach the higher
615 class, likely due to the longer residence times, i.e., a longer period before reaching equilibrium.

616 The average increase in groundwater [NO₃] over the Island for the four climate scenarios (2-5;
617 [Figures 7a-d](#)) range between 11 and 17% ([Table S1](#)) with respect to the present-day scenario
618 ([Figure 6a](#)). The departures from the baseline scenario suggest that the impact of groundwater
619 recharge change alone (without the equilibrium effect) on [NO₃] is 6% for CGCM2-A2 and
620 HadCM3-A2, 4% for HadCM3-B2, and zero for CGCM2-B2. There is thus also no significant
621 change in [NO₃] classes and only two watersheds moving from the low to the medium class for
622 all climate scenarios ([Figure 7a-d](#); [Table S1](#)). These simulations indicate that modification of the
623 groundwater recharge regime caused by climate change (scenarios 2-5) has less impact on future
624 water quality than reaching equilibrium with current nitrate mass (scenario 1).

625 The Island average concentration for each climate scenario integrating the agricultural adaptation
626 scenario (6 to 9; [Figures 8a-d](#)) indicates a nitrate increase between 25 and 32 % ([Table S1](#))
627 relative to the present-day simulation ([Figure 6a](#)). The scenarios with CGCM2-A2 (scenario 6,
628 [Figure 8a](#)) and HadCM3-A2 (scenario 8, [Figure 8c](#)) predict the highest impacts with 64% of the
629 watersheds in the medium (17) or the high (8) class, while the scenario with CGCM2-B2
630 (scenario 7, [Figure 8b](#)) has the lowest impact (58% in medium or high class). The center of the
631 Island is more strongly affected by high [NO₃], as expected from the intensification of
632 agricultural activities for the 2049-2069 period ([Figure 5b](#)). Moreover, the comparison of
633 scenarios 6 to 9 with the baseline scenario indicates that changes in agricultural practices (land
634 use and fertilization) and crop yields induced by climate change would have an impact on the
635 increase of average [NO₃] between 14 and 21% ([Table S1](#)). Thus agricultural adaptation will
636 potentially have a greater effect on future groundwater [NO₃] in PEI than groundwater recharge
637 change induced by climate change (0-6%) or the reach of [NO₃] equilibrium in the aquifer system
638 (11%).

639 Figure 6

640 Figure 7

641 Figure 8

642 5 Discussion

643 5.1 Comparison with Previous Studies

644 [De Jong et al. \(2008\)](#) document the only other study on the assessment of the impact of climate
645 and agricultural practice changes on groundwater quality for PEI. Similar to our study, they
646 showed that the impact of the projected climate change on N leaching is small compared to the
647 effect of agricultural intensification that could increase soil N leaching well above historical
648 levels. While they showed that there was a reasonable qualitative agreement between simulated N
649 leaching and groundwater [NO₃] in domestic wells, the sole simulation of N movement through
650 the unsaturated zone does not allow a quantitative assessment of the effect of the aquifer system
651 dynamics on [NO₃] in groundwater. Nevertheless, their simulations of N movement on a daily
652 basis during the non-growing season indicated that a few percentages of the RSN was not
653 reaching groundwater each year. On average, for all SLC polygons, 91% of the RSN was indeed
654 lost via soil leaching, with a range from 87 to 96% over the Island. In comparison, we assumed
655 that 100% of the RSN was reaching the aquifer system each year. On the other hand, [De Jong et al. \(2008\)](#)
656 neglected N leaching during the growing season, which is contradicted by the findings
657 of [Savard et al. \(2010\)](#) and [Ballard et al. \(2009\)](#), which showed important input of nitrate in
658 groundwater throughout the year, including during the growing season.

659 The results obtained for PEI can also be compared to those reported by [Ducharme et al. \(2007\)](#) for
660 the Seine basin (France). The main findings of this study are indeed similar to those obtained for
661 PEI. First, the dynamics of the aquifer system of the Seine basin leads to an important increase in
662 future [NO₃]. This increase is however at least twice the percentage obtained for PEI by 2050,
663 which suggests that the residence time of nitrate in the PEI aquifer system is shorter and it could
664 equilibrate faster to a change in nitrate mass. This could be explained by the different geology
665 between the two aquifer systems. For the Seine basin, the influence of climate on groundwater
666 recharge also has a minor impact on the increases of future [NO₃], as indicated by small to
667 moderated decreases in river low flows (baseflow), so the reason why climate change leads to
668 higher [NO₃] in groundwater is the increased nitrate leaching from the soils. This increased
669 leaching is mainly related to enhanced crop biomass and yield as well as soil N mineralization
670 (this process was not considered in our study). In our study, the increased nitrate leaching results
671 from larger agricultural land, increased fertilizer use and higher crop yield. Thus, future studies in
672 PEI should include a comprehensive simulation of nitrate movement through the unsaturated

673 zone with a consideration of soil N mineralization to be more representative of actual and future
674 agricultural conditions.

675 **5.2 Assessing Model Uncertainty through Calibration**

676 In this study, the proposed workflow includes numerous modelling steps, which involve many
677 hypotheses and conceptual choices. While a sensitivity analysis could be made on each of the
678 many model parameters to quantify and propagate the uncertainty on groundwater [NO₃]
679 predictions, the strength of our approach is rather to capitalize on known conditions that are used
680 in a comprehensive calibration approach that constrains the possible range of model parameters.
681 As reminded in [Figure 9](#), [NO₃] in groundwater depends on the mass of nitrate combined with the
682 amount of water reaching the water table and the mixing of that infiltration with the flowing
683 groundwater. Obviously, different combinations of nitrate mass, recharge and water flux could
684 lead to the same [NO₃], and at least two of the three parameters need to be independently
685 calibrated to obtain meaningful predictions of [NO₃] in groundwater. For this study, the flux of
686 water coming from the surface (groundwater recharge) and flowing within the aquifer system
687 were carefully calibrated with river baseflow and groundwater hydraulic head data. However, the
688 mass of nitrate applied at the soil surface through RSN estimates was more uncertain at the scale
689 investigated, and measurements in wells were instead used to calibrate [NO₃] in groundwater.
690 Thus, the estimated mass of nitrate and flux of water (recharge and within the aquifer system) are
691 likely representative of the actual conditions in PEI, and the performance of the FEFLOW model
692 to predict [NO₃] in groundwater could be used to quantify the uncertainty propagated during the
693 modelling process.

694 [Figure 9](#).

695 **5.3 Assessing Uncertainty in Future Predictions**

696 Uncertainties in the projections related to climate models and forcing scenarios could be large,
697 although the objectives of this study were to develop methodologies for assessing climate change
698 impacts on groundwater [NO₃] and demonstrate their application in PEI. Projected climate
699 changes by the two state-of-the-art GCMs, CanESM2 ([Arora et al., 2011](#)) and HadGEM2 ([Johns
700 et al., 2006](#); [Martin et al., 2006](#)), from the same climate modelling centres of CGCM2 and
701 HadCM3, are presented in [Table S2](#) under the Representative Concentration Pathways (RCP) 4.5

702 and 8.5. The projected temperature changes are larger in these new simulations. It is also noticed
703 that an increase in July precipitation by over 20% was projected with little change or a decrease
704 in the number of rainy days. Such changes could indicate increased precipitation intensity.

705 As reported by [De Jong et al. \(2008\)](#), N leaching in PEI is however considerably less sensitive to
706 increases in daily precipitation than to decreases. For instance, a 15% increase in annual
707 precipitation resulted in a 2.5% increase in N leaching, which is likely due to the high level of
708 soil water saturation throughout much of the year in this temperate-humid climate. Thus,
709 increased precipitation intensity could not result in a significant increase in N leaching to the
710 aquifer system because much of the excess water will drain as surface runoff. Nevertheless, the
711 projected groundwater [NO₃] under these new climate scenarios might differ from those based on
712 CGCM2 and HadCM3 and uncertainties in the projections should be taken into account when
713 results are used to develop adaptation strategies and policies.

714 Finally, while we considered only a single “worst case” agricultural adaptation scenario, it should
715 be understood that this scenario was designed to explore the upper limits of potential future
716 conditions. Thus, any adaptation strategy (e.g., better agricultural practices) will have to make
717 sure that such an upper limit is not actually reached. This study thus serves as an indicator of the
718 magnitude of the reduction needed on N leaching by agricultural adaptation strategies to
719 counteract the projected increase in [NO₃] in groundwater.

720 **6 Summary**

721 To assess the potential impact of climate change and the foreseen agricultural adaptation on
722 [NO₃] in groundwater over the PEI, nine different groundwater flow and mass transport scenarios
723 were considered. Simulations of these scenarios and their results expected for 2050 show that:

- 724 • The progressive change of groundwater [NO₃] simply due to reaching steady-state conditions
725 related to present-day loading would generate an 11% increase of concentrations.
- 726 • Groundwater recharge change related to climate change would only account for an increase
727 of 0 to 6%, whereas agricultural adaptation that include land use, fertilization and crop yield
728 changes induced by climate change would generate an increase of 14 to 21%.
- 729 • The combined effect of equilibration with loadings, groundwater recharge change and
730 agricultural adaptation would create an increase in [NO₃] between 25 and 32% over the PEI
731 aquifer system.

732 As a consequence, the predicted general trend from 2001 to 2050 is that a significant number of
733 watersheds would belong to the highly impacted group of watersheds having a mean [NO₃]
734 exceeding 5 mg/L (N-NO₃) with a recommended maximum concentration limit of 10 mg/L (N-
735 NO₃) for drinking water. In 2001, 4 watersheds over a total of 50 were in this group compared to
736 8 predicted for 2050 after reaching steady-state conditions and having undergone some of the
737 climate change, or 9 to 11 after agricultural adaptation is also considered.

738 Finally, predicting the impact of climate change on groundwater quality in agricultural contexts
739 represents a complex challenge that we have attempted to address using the case study of PEI. In
740 that particular example, the main finding in support to decision making for sustainable
741 development is that predicted climatic conditions combined with agricultural practices adapted to
742 these conditions may be expected to generate significant degradation of water quality that would
743 require modifying water servicing infrastructures, and develop better agricultural management
744 practices to reduce nitrate leaching to the aquifer system (e.g., [Zebarth et al., 2015](#); [Somers and
745 Savard, 2015](#)). At a broader scale, we also have made progress in pinpointing key steps to be
746 considered in predictive modelling, particularly in highlighting the need to produce sound and
747 realistic scenarios of region-specific agricultural adaptation to climate change while considering
748 the specificity of the hydrogeological processes taking place, and applying a comprehensive
749 calibration process to narrow the uncertainty in model parameters and results.

750 **Acknowledgements**

751 This study was funded by Natural Resources Canada (Climate Change Impact and Adaptation),
752 and the Geological Survey of Canada (Groundwater Program). [The authors are grateful to A.
753 Shepard and M. Vanclooster for their constructive reviews and to the Editor M. Crucifix.](#) A
754 NSERC Discovery Grant also supported RL. This is an ESS contribution [20150425](#).

755 **References**

- 756 Allen, D. M., Mackie, D. C., and Wei, M.: Groundwater and climate change: a sensitivity
757 analysis for the Grand Forks aquifer, southern British Columbia, Canada, *Hydrogeol. J.*, 12, 270-
758 290, 2004.
- 759 Allen, D. M., Cannon, A. J., Toews, M. W., and Scibek, J.: Variability in simulated recharge
760 using different GCMs, *Water Resour. Res.*, 46, W00F03, doi:10.1029/2009WR008932, 2010.

761 Arora, V. K., Scinocca, J. F., Boer, G. J., Christian, J. R., Denman, K. L., Flato, G. M., Kharin,
762 V. V., Lee, W. G., and Merryfield, W. J.: Carbon emission limits required to satisfy future
763 representative concentration pathways of greenhouse gases, *Geophys. Res. Lett.*, 38, 2011.

764 Ballard, J.-M., Paradis, D., Lefebvre, R., and Savard, M. M.: Numerical modeling of the
765 dynamics of multisource nitrate generation and transfer, PEI, GeoHalifax '09, 62th Canadian
766 Geotechnical Conference and 10th Joint CGS/IAH Conference, Halifax, Canada, September 20-
767 24, 2009, Paper 210, 1507-1514, 2009.

768 Beigi, E., and Tsai, F. T.-C.: Comparative study of climate-change scenarios on groundwater
769 recharge, southwestern Mississippi and southeastern Louisiana, USA, *Hydrogeol. J.*, 23, 789-806,
770 2015.

771 Bootsma, A., Gameda, S., McKenney, D. W.: Adaptation of agricultural production to climate
772 change in Atlantic Canada, Final report for Climate Change Action Fund Project A214, 30 p.,
773 2001.

774 Burns, D. A., Klaus, J., and McHale, M. R.: Recent climate trends and implications for water
775 resources in the Catskill Mountain region, New York, USA, *J. Hydrol.*, 336, 155-170, 2007.

776 Burton, D. L., and Beauchamp, E. G.: Nitrogen losses from swine housings, *Agric. Waste*, 15,
777 59-74, 1986.

778 CanImage : Landsat-7 Ortho-Images of Canada, 1/50000, Prince Edward Island, 2001.

779 Canadian Soil Information System: National Soil Database, Agriculture and Agri-Food Canada,
780 2000.

781 Crosbie, R. S., McCallum, J. L., Walker, G. R., and Chiew, F. H. S. : Modelling climate-change
782 impacts on groundwater recharge in the Murray-Darling Basin, Australia, *Hydrogeol. J.*, 18,
783 1639-1656, 2010.

784 Croteau, A., Nastev, M., and Lefebvre, R.: Groundwater recharge assessment in the Chateauguay
785 River watershed, *Can. Water Resour. J.*, 35(4), 451-468, 2010.

786 De Jong, R., Qian, B., and Yang, J. Y.: Modelling nitrogen leaching in Prince Edward Island
787 under Climate change scenarios, *Can. J. Soil Sci.*, 88, 61-78, 2008.

788 Diersch, H.-J. G.: FEFLOW: Finite Element Subsurface Flow and Transport Simulation System-
789 Reference Manual, v.6.0. WASY GmbH Software Berlin, 277 p., 2010.

790 Drury, C. F., Yang, J. Y., De Jong, R., Yang, X. M., Huffman, E., Kirkwood, V., and Reid, K.:
791 Residual soil nitrogen indicator for Canada, *Can. J. Soil Sci.*, 87, 166-177, 2007.

792 Ducharne, A., Baubion, C., Beaudoin, N., Benoit, M., Billen, G., Brisson, N., Garnier, J., Kieken,
793 H., Lebonvallet, S., Ledoux, E., Mary, B., Mignolet, C., Poux, X., Sauboua, E., Schott, C., Théry,
794 S., Viennot, P.: Long term prospective of the Seine River system: Confronting climatic and direct
795 anthropogenic changes, *Sci. Tot. Environ.*, 375, 292-311, 2007.

796 Flato, G. M., and Boer, G. J.: Warming Asymmetry in Climate Change Simulations, *Geoph. Res.*
797 *Let.*, 28, 195-198, 2001.

798 Francis, R. M.: Hydrogeology of the Winter River Basin, Prince Edward Island, Department of
799 the Environment, Water Resources Branch, Prince Edward Island, 117 p., 1989.

800 Furey, P. R., and Gupta, V. K.: A physically based filter for separating base flow from
801 streamflow time series, *Water Resour. Res.*, 37, 11, 2709-2722, 2001.

802 Gelhar, L. W., Welty, C., and Rehfeldt, K. R.: A critical review of data on field-scale dispersion
803 in aquifers, *Water Resour. Res.*, 28, 7, 1955-1974, 1992.

804 Ghiglieri, G., Barbieri, G., Vernier, A., Carletti, A., Demurtas, N., Pinna, R., and Pittalis, D.:
805 Potential risks of nitrate pollution in aquifers from agricultural practices in the Nurra region,
806 northwestern Sardinia, Italy, *J. Hydrol.*, 379, 339-350, 2010.

807 Gleick, P. H.: Methods for evaluating the regional hydrologic impacts of global climatic changes,
808 *J. Hydrol.*, 88, 91-116, 1986.

809 Gordon, C., Cooper, C., Senior, C. A., Banks, H., Gregory, J. M., Johns, T. C., Mitchell, J. F. B.,
810 and Wood, R. A.: The simulation of SST, sea ice extents and ocean heat transports in a version of
811 the Hadley Centre coupled model without flux adjustments, *Clim. Dyna.*, 16, 147-168, 2000.

812 Green, T. R., Taniguchi, M., and Kooi, H.: Potential impacts of climate change and human
813 activity on subsurface water resources, *Vadose Zone J.*, 6, 531-532, 2007a.

814 Green, T. R., Bates, B. C., Charles, S. P., and Fleming, P. M.: Physically based simulation of
815 potential effects of carbon dioxide altered climates on groundwater recharge, *Vadose Zone J.*, 6,
816 597-609, 2007b.

817 Hagg, W., Braun, L. N., Huhn, M., and Nesgaard, T. I.: Modelling of hydrological response to
818 climate change in glacierized Central Asia catchments, *J. Hydrol.*, 332, 40-53, 2007.

819 Hayhoe, H. N.: Improvements of stochastic weather data generators for diverse climates, *Climate*
820 *Res.*, 14, 75-87, 2000.

821 Health Canada: Summary of guidelines for Canadian drinking water quality, Prepared by the
822 Federal-Provincial-Territorial Committee on Drinking Water of the Federal-Provincial-
823 Territorial Committee on Health and the Environment, <http://www.hc-sc.gc.ca/waterquality>,
824 2004.

825 Hengeveld, H. G.: Projections for Canada's climate future: A discussion of recent simulations
826 with the Canadian global climate model, Science Assessment and Integration Branch,
827 Meteorological Service of Canada, Downsview, Ontario, Canada, 27 p., 2000.

828 Holman, I. P., Rounsevell, M. D. A., Shackley, S., Harrison, P. A., Nicholls, R. J., Berry, P. M.,
829 and Audsley, E.,: A regional, multi-sectoral and integrated assessment of the impacts of climate
830 and socio-economic change in the UK: Part 1 Methodology, *Clim. Change*, 71, 9-41, 2005a.

831 Holman, I. P., Nicholls, R. J., Berry, P. M., Harrison, P. A., Audsley, E., Shackley, S., and
832 Rounsevell, M. D. A.: A regional, multi-sectoral and integrated assessment of the impacts of
833 climate and socio-economic change in the UK: Part 2 Results, *Clim. Change*, 71, 43-73, 2005b.

834 Holman, I. P., Tascone, D., and Hess, T. M.: A comparison of stochastic and deterministic
835 downscaling methods for modelling potential groundwater recharge under climate change in East
836 Anglia, UK: implications for groundwater resource management, *Hydrogeol. J.*, 17, 1629-1641,
837 2009.

838 Hsu, K.-C., Wang, C.-H., Cheu, K.-C., Chen, C.-T., and Ma, K.-W.: Climate-induced
839 hydrological impacts on the groundwater system of the Pingtung Plain, Taiwan, *Hydrogeol. J.*,
840 15, 903-913, 2007.

841 Huffman, T., Ogston, R., Fisette, T., Daneshfar, B., Gasser, P. Y., White, L., Maloley, M., and
842 Chenier, R.: Canadian agricultural land-use and land management data for Kyoto reporting, Can.
843 J. Soil Sci., 86, 431-439, 2006.

844 International Panel on Climate Change (IPCC): Climate Change 2001-Working Group I: The
845 Scientific Basis, http://www.grida.no/climate/ipcc_tar/wg1/index.htm, 2001.

846 Jackson, B. M., Wheeler, H. S., Wade, A. J., Butterfield, D., Mathias, S. A., Ireson, A. M.,
847 Butler, A. P., McIntyre, N. R., and Whitehead, P.G.: Catchment-scale modelling of flow and
848 nutrient transport in the Chalk unsaturated zone, Ecol. Model, 209, 41-52, 2007.

849 Jiang, Y., and Somers, G.: Modeling effects of nitrate from non-point sources on groundwater
850 quality in an agricultural watershed in Prince Edward Island, Canada, Hydrogeol. J., 17, 707-724,
851 2009.

852 Johns, T. C., Durman, C. F., Banks, H. T., Roberts, M. J., McLaren, A. J., Ridley, J. K., Senior,
853 C. A., Williams, K. D., Jones, A., Rickard, G. J., Cusack, S., Ingram, W. J., Crucifix, M., Sexton,
854 D. M. H., Joshi, M. M., Dong, B. W., Spencer, H., Hill, R. S. R., Gregory, J. M., Keen, A. B.,
855 Pardaens, A. K., Lowe, J. A., Bodas-Salcedo, A., Stark, S., and Searl, Y.: 2006. The new Hadley
856 Centre Climate Model (HadGEM1): Evaluation of coupled simulations, J. Clim., 19, 1327-1353,
857 2006.

858 Jyrkama, M. I., Sykes, J. F., and Normani, S. D.: Recharge estimation for transient ground water
859 modelling, Ground Water, 40, 6, 638-648, 2002.

860 Jyrkama, M. I., and Sykes, J. F.: The impact of climate change on spatially varying groundwater
861 recharge in the grand river watershed (Ontario), J. Hydrol., 338, 237-250, 2007.

862 Martin, G. M., Ringer, M. A., Pope, V. D., Jones, A., Dearden, C., and Hinton, T. J., The
863 physical properties of the atmosphere in the new Hadley Centre Global Environmental Model
864 (HadGEM1). Part I: Model description and global climatology, J. Clim., 19, 1274-1301, 2006.

865 McCallum, J. L., Crosbie, R. S., Walker, G. R., and Dawes, W. R. : Impacts of climate change on
866 groundwater in Australia: a sensitivity analysis of recharge, Hydrogeol. J., 18, 1625-1638, 2010.

867 McGinn, S. M., and Shepherd, A.: Impact of climate change scenarios on the agroclimate of the
868 Canadian prairies, Can. J. Soil Sci., 83, 623-630, 2003.

869 Mendoza, G. F., Steenhuis, T. S., Walter, M. T., and Parlange, J. Y.: Estimating basin-wide
870 hydraulic parameters of a semi-arid mountainous watershed by recession-flow analysis, *J.*
871 *Hydrol.*, 279, 57-69, doi:10.1016/S0022-1694(03)00174-4, 2003.

872 Monfet, J.: Évaluation du coefficient de ruissellement à l'aide de la méthode SCS modifiée,
873 Service de l'hydrométrie, Ministère des Richesses Naturelles, Gouvernement du Québec,
874 Publication HP-51, 35 p. 1979.

875 Mutch, J.: The hydrologic cycle and water movement, Nitrate-agricultural sources and fate in the
876 environment-perspectives and direction. Proceedings of the workshop, Eastern Canada Soil and
877 Water Conservation Centre, p. 3-7, 1998.

878 Nakicenovic, N., and Swart, R.: Special Report on Emissions Scenarios-A special report of
879 Working Group III of the Intergovernmental Panel on Climate Change, Cambridge University
880 Press, Cambridge, UK, 612 p., 2000.

881 Okkonen, J., Jyrkama, M., and Kløve, B.: A conceptual approach for assessing the impact of
882 climate change on groundwater and related surface waters in cold regions (Finland), *Hydrogeol.*
883 *J.*, 18, 429-439, 2010.

884 Olesen, J. E., and Bindi, M.: Consequences of climate change for European agricultural
885 productivity, land use and policy, *Eur. J. of Agron.*, 16, 239-262, 2002.

886 Ontario Ministry of Agriculture and Food: Soil fertility handbook, Publication 611, Ontario
887 Ministry of Agriculture and Food, 2003.

888 Paradis, D., Ballard, J.-M., Savard, M. M., Lefebvre, R., Jiang, Y., Somers, G., Shawna, L., and
889 Rivard, C.: Impact of agricultural activities on nitrate in ground and surface water in the Wilmot
890 Watershed, PEI, Canada, Proceedings, 59th Canadian Geotechnical Conference and 7th Joint
891 CGS/IAH Conference, Vancouver, Canada, October 1-4, 2006, Paper 244, 8 p., 2006.

892 Paradis, D., Ballard, J.-M., and Lefebvre, R.: Watershed scale numerical modelling of nitrate fate
893 and transport using spatially uniform averaged N-inputs, In: Savard, M. M. and Somers, G.
894 (Editors), Consequences of climatic changes on contamination of drinking water by nitrates on
895 Prince Edward Island. Report of the Climate Change Action Fund: Impacts and Adaptation
896 (A881/A843), Natural Resources Canada, 49-62, 2007.

- 897 Prest, V. K.: Surficial deposits of Prince Edward Island, Geological Survey of Canada, A-Series
898 Map 1366A, 1973.
- 899 Qian, B., Gameda, S.B., De Jong, R., Falloon, P.D., et Gornall, J.: Comparing scenarios of
900 Canadian daily climate extremes derived using a weather generator, *Clim. Res.*, 41, 2, 131-149,
901 doi : 10.3354/cr00845, 2010.
- 902 Qian, B., De Jong, R., Yang, J., Wang, H., Gameda, S.: Comparing simulated crop yields with
903 observed and synthetic weather data, *Agricultural and Forest Meteorology*, 151, 12, 15, 1781-
904 1791, <http://dx.doi.org/10.1016/j.agrformet.2011.07.016>, 2011.
- 905 Qian, B. D., Gameda, S., Hayhoe, H., De Jong, R., and Bootsma, A.: Comparison of LARS-WG
906 and AAFC-WG stochastic weather generators for diverse Canadian climates, *Clim. Res.*, 26, 3,
907 175-191, 2004.
- 908 Qian, B., and De Jong, R.: Modelling four Climate change scenarios for Prince Edward Island,
909 In: Savard, M. M. and Somers, G. (Editors), *Consequences of climatic changes on contamination*
910 *of drinking water by nitrates on Prince Edward Island. Report of the Climate Change Action*
911 *Fund: Impacts and Adaptation (A881/A843)*, Natural Resources Canada, 63-71, 2007.
- 912 Risser, D. W., Gburek, W. J., and Folmar, G. J.: Comparison of methods for estimating
913 groundwater recharge and base flow at a small watershed underlain by fractured bedrock in the
914 eastern United States, *USGS Scientific Investigations Report 2005-5038*, 31 p., 2005.
- 915 Rivard, C., Lefebvre, R., and Paradis, D.: Regional recharge estimation using multiple methods:
916 an application in the Annapolis Valley, Nova Scotia (Canada). *Environmental Earth Sciences*,
917 71(3), 1389–1408, 2014.
- 918 Rivard, C., Vigneault, H., Piggott, A. R., Larocque, M., and Anctil, F.: Groundwater recharge
919 trends in Canada, *Can. J. Earth Sci.*, 46, 841-854, 2009.
- 920 Rivard, C., Paradis, D., Paradis, S. J. , Bolduc, A., Morin, R. H., Liao, S. L, Pullan, S., Gauthier,
921 M. J., Trépanier, S., Blackmore, A., Spooner, I., Deblonde, C., Fernandes, R., Castonguay, S.,
922 Michaud, Y., Drage, J., and Paniconi, C.: Canadian groundwater inventory: Regional
923 hydrogeological characterization of the Annapolis-Cornwallis Valley aquifers, *GSC Bulletin 589*,
924 86 p., 2008.

- 925 Rozell, D. J., and Wong, T.-F.: Effects of climate change on groundwater resources at Shelter
926 Island, New York State, USA, *Hydrogeol. J.*, 18, 657-1665, 2010.
- 927 Ruth, M., Bernier, C., Jollands, N., and Golubieswski. N.: Adaptation of urban water supply
928 infrastructure to impacts from climate and socioeconomic changes: the case of Hamilton, New
929 Zealand, *Water Resour. Manag.*, 21, 1013-1045, 2007.
- 930 Sánchez-Murillo, R., Brooks, E. S., Elliot, W. J., Gazel, E., and Boll, J.: Baseflow recession
931 analysis in the inland Pacific Northwest of the United States, *Hydrogeol. J.*, 23, 2, 287-303,
932 doi/10.1007/s10040-014-1191-4, 2015.
- 933 Savard, M. M., Paradis, D., Somers, G., Liao, S., and van Bochove, E.: Winter nitrification
934 contributes to excess NO_3^- in groundwater of an agricultural region: A dual-isotope study, *Water*
935 *Resour. Res.*, 43, W06422, doi:10.1029/2006WR005469, 2007.
- 936 Savard, M. M., Somers, G., Smirnoff, A., Paradis, D., van Bochove, E., and Liao, S.: Nitrate
937 isotopes unveil distinct seasonal N-sources and the critical role of crop residues in groundwater
938 contamination, *J. Hydrol.*, 381, 134-141, 2010.
- 939 Savard, M. M., and Somers, G., ed.: Consequences of climatic changes on contamination of
940 drinking water by nitrates on Prince-Edward-Island. Geological Survey of Canada, Agriculture
941 and Agri-Food Canada, PEI Environment, Energy & Forestry, Report to Natural Resources
942 Canada, Climate Change Action Fund: Impacts & Adaptation, Contribution A881/A843, March
943 20, 2007.
- 944 Schroeder, P. R., Aziz, N. M., Lloyd, C. M., and Zappi, P. A.: The hydrologic evaluation of
945 landfill performance (HELP) model, Engineering documentation for version EPA/600/R-
946 94/168b, 116 p., 1994.
- 947 Scibek, J., and Allen, D. M.: Modeled impacts of predicted climate change on recharge and
948 groundwater levels, *Water Resour. Res.*, 42, W11405, doi:10.1029/2005WR004742, 2006.
- 949 Serrat-Capdevila, A., Valdés, J. B., González Pérez, J., Baird, K., Mata, L. J., and Maddock III,
950 T.: Modeling climate change impacts and uncertainty on the hydrology of a riparian system: the
951 San Pedro Basin (Arizona/Sonora), *J. Hydrol.*, 347, 48-66, 2007.

952 Soil Landscapes of Canada Working Group: Soil Landscapes of Canada v3.1, Agriculture and
953 Agri-Food Canada (digital map and database at 1:1 million scale), 2006.

954 Somers, G.: Distribution and trends for occurrence of nitrate in PEI groundwater, In: Proc. from
955 nitrate-agricultural sources and fate in the Environment-Perspectives and Direction, Grand Falls,
956 Canada, 1998.

957 Somers, G., and Mutch, J.: Results of an investigation into the impact of irrigation wells on the
958 availability of groundwater in the Baltic area, <http://res.agr.ca/cansis/nsdb/slc/v3.1/intro.html>,
959 1999.

960 Somers, G. H., Raymond, B., and Uhlman, W.: Prince Edward Island water quality interpretative,
961 Report 99 prepared for Canada-Prince Edward Island Water Annex to Federal/Provincial
962 Framework Agreement for Environmental Cooperation in Atlantic Canada, 67 p., 1999.

963 Somers, G., Savard, M.M.: Shorter fries? An alternative policy to support a reduction of nitrogen
964 contamination from agricultural crop production. *J. Env. Sci. & Policy*, 47, 177-185, 2015.

965 Tóth, J.: A theoretical analysis of groundwater flow in small drainage basins, *J. Geophys. Res.*,
966 68,16, 4795-4812, 1963.

967 United States Department of Agriculture (USDA): Urban hydrology for small watersheds, Soil
968 Conservation Service, Engineering Division, Technical Release 55 (TR-55), 1986.

969 Van de Poll, H. W.: Geology of Prince Edward Island, Prince Edward Island Department of
970 Energy and Forestry, Energy and Minerals Branch, Charlottetown, 66 p., 1983.

971 Woldeamlak, S. T., Batelaan, O. and De Smedt, F.: Effects of climate change on the groundwater
972 system in the Grote-Nete catchment, Belgium, *Hydrogeol. J.*, 15, 891-901, 2007.

973 Yang, J. Y., De Jong, R., Drury, C. F., Huffman, E. C., Kirkwood, V., and Yang, X. M.:
974 Development of a Canadian agricultural nitrogen budget model (CANB v2.0): Simulation of the
975 nitrogen indicators and integrated modelling for policy scenarios, *Can. J. Soil Sci.*, 87, 153-165,
976 2007.

977 Young, J., Somers, G. H., Raymond, G. B.: Distribution and trends for nitrate in PEI groundwater
978 and surface waters, In: Proc. of National Conference on Agriculture Nutrients and their impact on

979 Rural Water Quality, April 29-30, 2002, Waterloo, Ontario, Agricultural Institute of Canada
980 Foundation, 313-319, 2002.

981 Yusoff, I., Hiscock, H. D., and Conway, D.: Simulation of the impacts of climate change on
982 groundwater resources in eastern England, Sustainable Groundwater Development. Geol. Soc.
983 Spec. Publ., 193, 325-344, 2002.

984 Zebarth, B. J., Danielescu, S., Nyiraneza, J., Ryan, M. C., Jiang, Y., Grimmett, M. G., and
985 Burton, D. L.: Controls on nitrate loading and implications for BMPs under intensive potato
986 production systems in Prince Edward Island, Canada, Ground Water Monit. R., 35, 30-42,
987 doi:10.1111/gwmmr.12088, 2015.

988 Zhou, Y., Zwahlen, F., Wang, Y., and Li, Y.: Impact of climate change on irrigation requirements
989 in terms of groundwater resources, Hydrogeol. J., 18, 1571-1582, 2010.

990

991

992 Table 1. Main physiographic and land use characteristics of Prince Edward Island (land use based
993 on a LANDSAT image for 2000).

Physiography	
Area	5 660 km ²
Width	3-65 km
Length	225 km
Elevation (above sea level)	0-140 m
Land Use (%)	
Forest	45
Agriculture	39
Wetland	7
Residential, urban, industrial	5.9
Recreational	0.3
Miscellaneous	2.8

994

995 Table 2. Weather for Prince Edward Island (meteorological data for the 1971-2000 period). See
 996 [Figure 1](#) for locations of the weather stations.

Weather Characteristic	Station			
	O'Leary	Summerside	Charlottetown	Monticello
Mean annual total precipitation (mm)	1141	1078	1173	1164
Mean annual rain (mm)	860	806	880	903
Mean annual snow (mm)	281	282	311	261
Mean annual temperature (°C)	5.2	5.6	5.3	5.5
Minimum mean monthly temperature (°C) (January)	-8.6	-7.9	-8.0	-7.4
Maximum mean monthly temperature (°C) (July)	18.5	19.1	18.5	18.4

997

998 Table 3. Streamflow characteristics of selected rivers in Prince Edward Island (records are for
 999 1972 to 2005, 1961 to 1995 and 1965 to 1991 for Wilmot, Morell, and Winter rivers,
 1000 respectively). See [Figure 1](#) for locations of the rivers.

Streamflow Characteristics (m ³ /s)	Watershed (drainage area in km ²)		
	Morell (133)	Wilmot (45)	Winter (38)
Mean annual	2.88	0.92	0.66
Minimum monthly mean (Sept.)	1.10	0.44	0.24
Maximum monthly mean (April)	6.77	1.89	1.61

1001

1002

1003

1004 Table 4. Statistical analysis of model performance on calibration of different independent data
1005 sets for the simulation of groundwater flow and nitrate transport in the Prince Edward Island
1006 aquifer system.

Model	Calibration Target	Model Error		
		Correlation Coefficient (r)	Relative Error (Bias in %)	Root Mean Square Error (RMS in %)
HELP	Groundwater recharge from baseflow	0.64	0.8	19
FEFLOW	Hydraulic head in open wells	0.88	-66.8	46
FEFLOW	Baseflow recession in rivers	0.96	0.3	3
FEFLOW	Nitrate concentration in wells	0.64	-0.3	30

1007

1008

1009 Table 5. Field-based and calibrated hydraulic properties of the FEFLOW numerical model for the
 1010 Prince Edward Island aquifer system.

Model Layer (depth in m)	Field K_h (m/s)	Numerical Model			
		K_h (m/s)	K_v/K_h (-)	S_y (%)	n (%)
1 (0-5)		3×10^{-4}	0.1	1	17
2 (5-10)	4.5×10^{-4} to 8.1×10^{-5}	1×10^{-4}	0.1	1	17
3 (10-15)		5×10^{-5}	0.1	1	17
4 (15-30)	1.7×10^{-4} to 8.4×10^{-7}	1×10^{-5}	0.01	1	17
5 (30-80)		1×10^{-5}	0.001	0.1	17
6 (80-180)	n.d.	1×10^{-6}	0.01	0.1	17
7 (180-380)	n.d.	1×10^{-7}	0.1	0.1	17
8 (380-880)	n.d.	1×10^{-8}	1	0.01	17

1011 K_h and K_v : are horizontal and vertical hydraulic conductivity, respectively; S_y : specific yield; n : total porosity

1012 Table 6. Temperature and precipitation changes for the future period (2040-2069) relative to the
 1013 historical period (1971-2000) for each selected climate change scenarios at the Charlottetown
 1014 weather station, Prince Edward Island (Qian and De Jong, 2007).

Scenario	Temperature change				Precipitation change			
	Monthly Mean Maximum (°C)		Monthly Mean Minimum (°C)		Monthly Total (%)		Days with Precipitation (%)	
	Jan.	July	Jan.	July	Jan.	July	Jan.	July
CGCM2-A2	1.7	2.5	4.6	3.1	-5.3	0.0	-2.1	5.0
CGCM2-B2	1.1	1.8	4.0	2.2	-8.1	5.0	-3.8	1.8
HadCM3-A2	1.4	1.8	1.7	2.0	4.1	7.7	-5.0	-4.6
HadCM3-B2	1.2	1.4	1.5	1.5	5.1	1.4	-3.0	-1.9

1015

1016

1017 Table 7. Summary of mean annual temperature and hydrologic cycle components (precipitation,
1018 evapotranspiration, surface runoff and groundwater recharge) simulated with the HELP model for
1019 the historical period (1970-2001) and the four climate scenarios (2040-2069) in Prince Edward
1020 Island. Values provided in brackets are the change in mm or °C for the 2040-2069 period
1021 compared to historical conditions (1970-2001).

Scenario	Temperature (°C)	Precipitation (mm)	Evapo- transpiration (mm)	Runoff (mm)	Recharge (mm)
Historic	5.3	1173	583	221	369
CGCM2-A2	8.0 (+3.31)	1109 (-64)	618 (+35)	155 (-66)	336 (-33)
CGCM2-B2	7.0 (+2.3)	1223 (+50)	620 (+37)	209 (-12)	394 (+25)
HadCM3-A2	6.7 (+1.4)	1141 (-32)	616 (+33)	202 (-19)	323 (-46)
HadCM3-B2	7.1 (+1.8)	1197 (+24)	615 (+32)	221 (0)	361 (-8)

1022

1023

1024

Table 8. Average components of the nitrogen balance as simulated with historical crop and animal husbandry practices and with an adapted agricultural management scenario (De Jong et

1025

1026

al., 2008).

Period	Nitrogen Inputs (kg N/ha/yr)						RSN (kg N/ha/yr)
	Fertilizer	Manure	Fixation	Deposition	Crop	Gas	
Historical	52.8	17.4	29.6	2.5	70.3	1.2	30.8
Adapted	61.2	16.8	30.1	2.5	73.2	1.6	35.7

1027

RSN: residual soil nitrogen.

1028

1029 **Figure Captions**

1030 Figure 1. (a) Location of Prince Edward Island (PEI) in eastern Canada. (b) Limits of the
1031 watersheds (numbered area delineated with brown lines, see names Table S1), with identification
1032 of the major rivers (names in blue), along with land use (see legend) and location of the weather
1033 stations (names in black).

1034 Figure 2. (a) Schematic conceptual model of the groundwater flow system along with (b) a
1035 typical profile of hydraulic conductivity showing distinct shallow high-flow (red) and deeper
1036 low-flow (blue) systems; and (c) a conceptualization of nitrate transport in the double-porosity
1037 sandstone aquifer with advective fracture flow and matrix diffusion.

1038 Figure 3. Workflow for the study of the potential impact of climate and agricultural practice
1039 changes on future groundwater nitrate concentration in the Prince Edward Island aquifer system.

1040 Figure 4. Spatial distribution of groundwater recharge from simulations with the calibrated HELP
1041 infiltration model for the historical period (1970-2001). Cell values are averages for the 1970-
1042 2001 period. Groundwater recharge is not shown for the 2040-2069 period as no significant
1043 changes were obtained from HELP based on climate change scenarios.

1044 Figure 5. Simulated residual soil nitrogen (RSN) using (a) historical management practices and
1045 (b) the adaptation scenario presented in [Table 8 \(De Jong et al., 2008\)](#). RSN values are for each
1046 Soil Landscape of Canada (SLC) polygon.

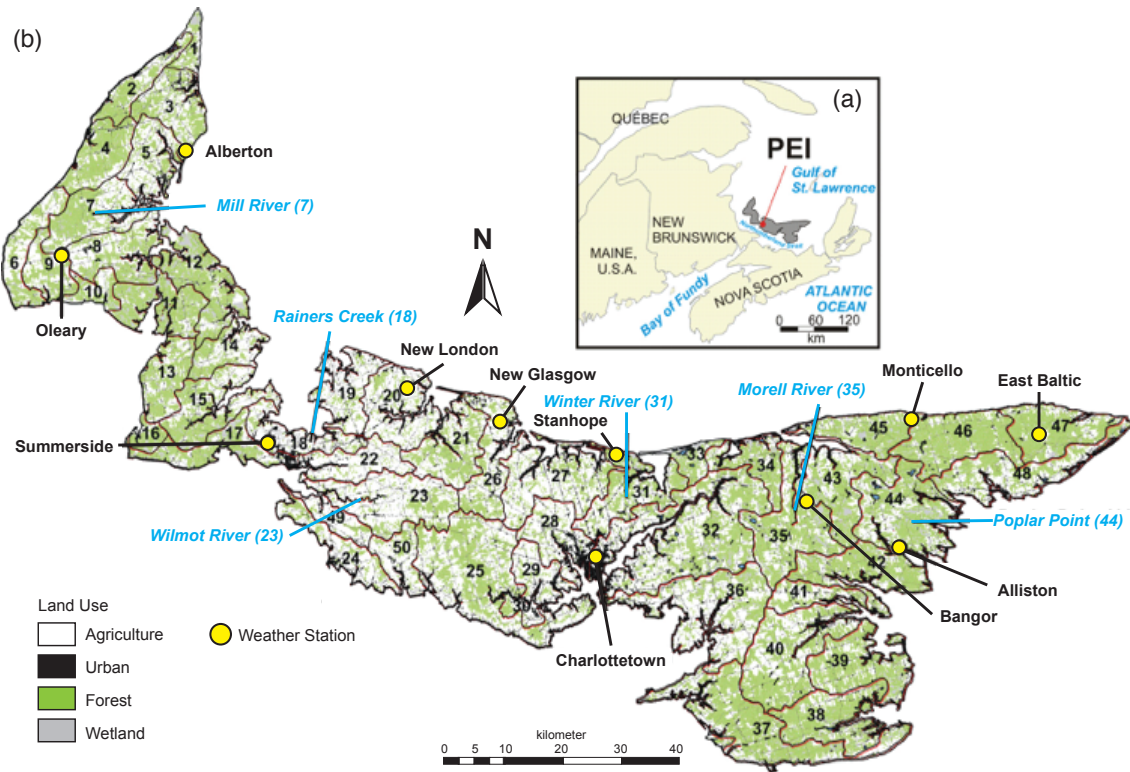
1047 Figure 6. Class distribution of simulated mean nitrate concentration per watershed and histogram
1048 of the number of watersheds in each class for: (a) present-day (2001); (b) 2050 baseline scenario
1049 with present-day (2001) nitrate loading and groundwater recharge.

1050 Figure 7. Class distribution of simulated mean nitrate concentration per watershed and histogram
1051 of the number of watersheds in each class for the four climate change (CC) scenarios (a, b, c and
1052 d).

1053 Figure 8. Class distribution of simulated mean nitrate concentration per watershed and histogram
1054 of the number of watersheds in each class for the four climate change (CC) scenarios with
1055 ensuing agricultural practice adaptation (APC) (a, b, c and d).

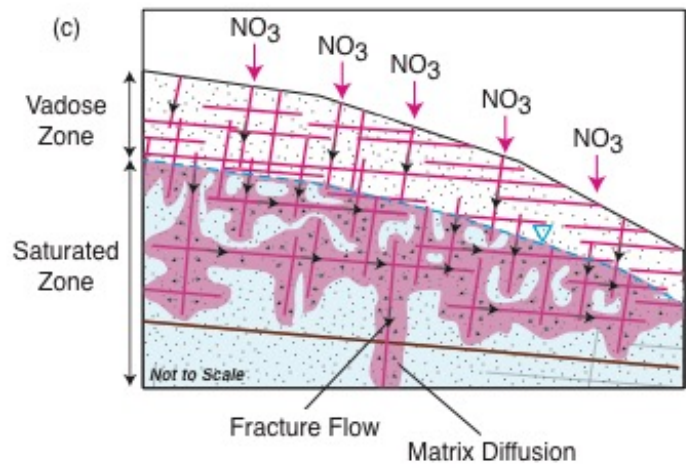
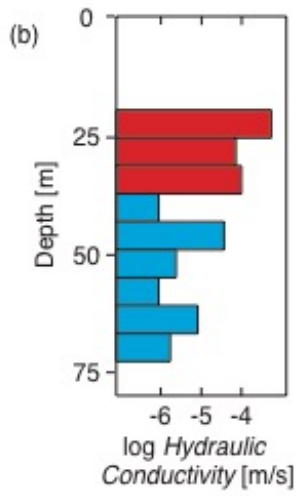
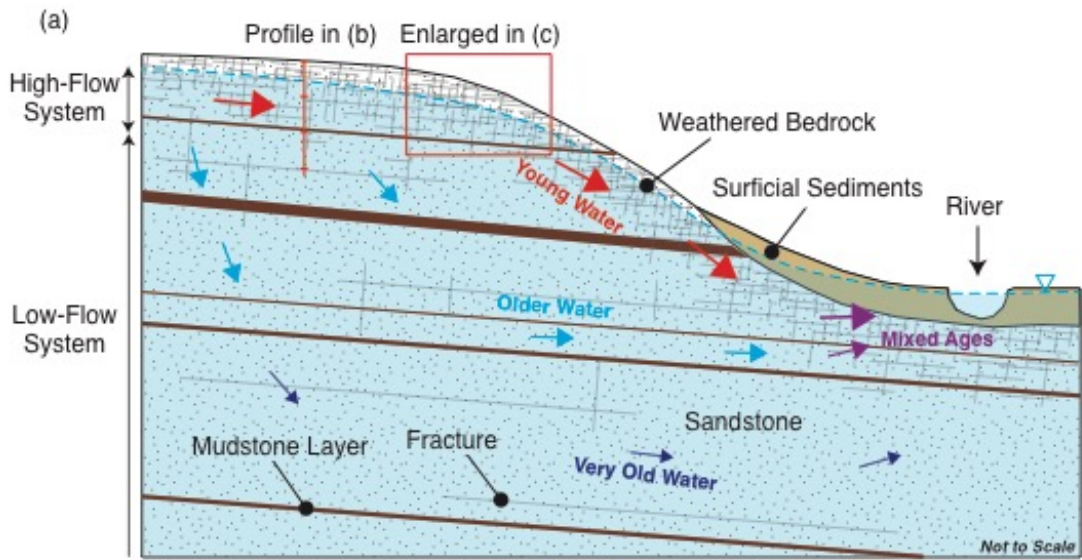
1056 Figure 9. Schematic of the constraints exerted by conditions considered (in blue) in the
1057 calibration of model parameters for the simulation of processes controlling groundwater nitrate
1058 concentration (NO_3 mass leached and water fluxes, including recharge and groundwater flow).

1059



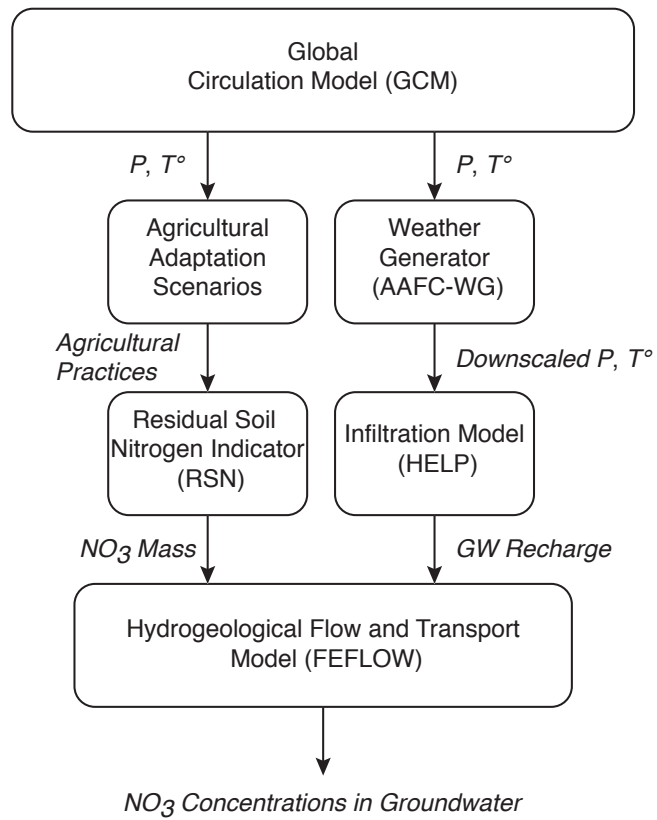
1060

1061



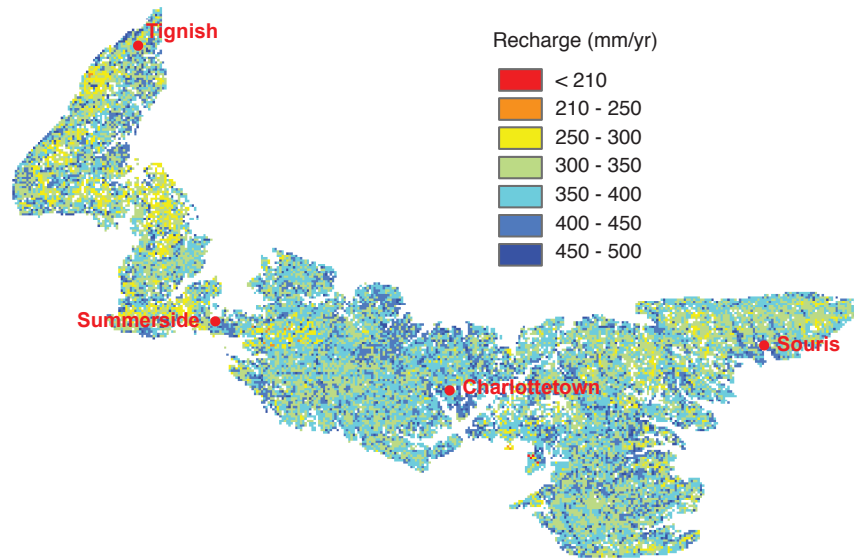
1062

1063



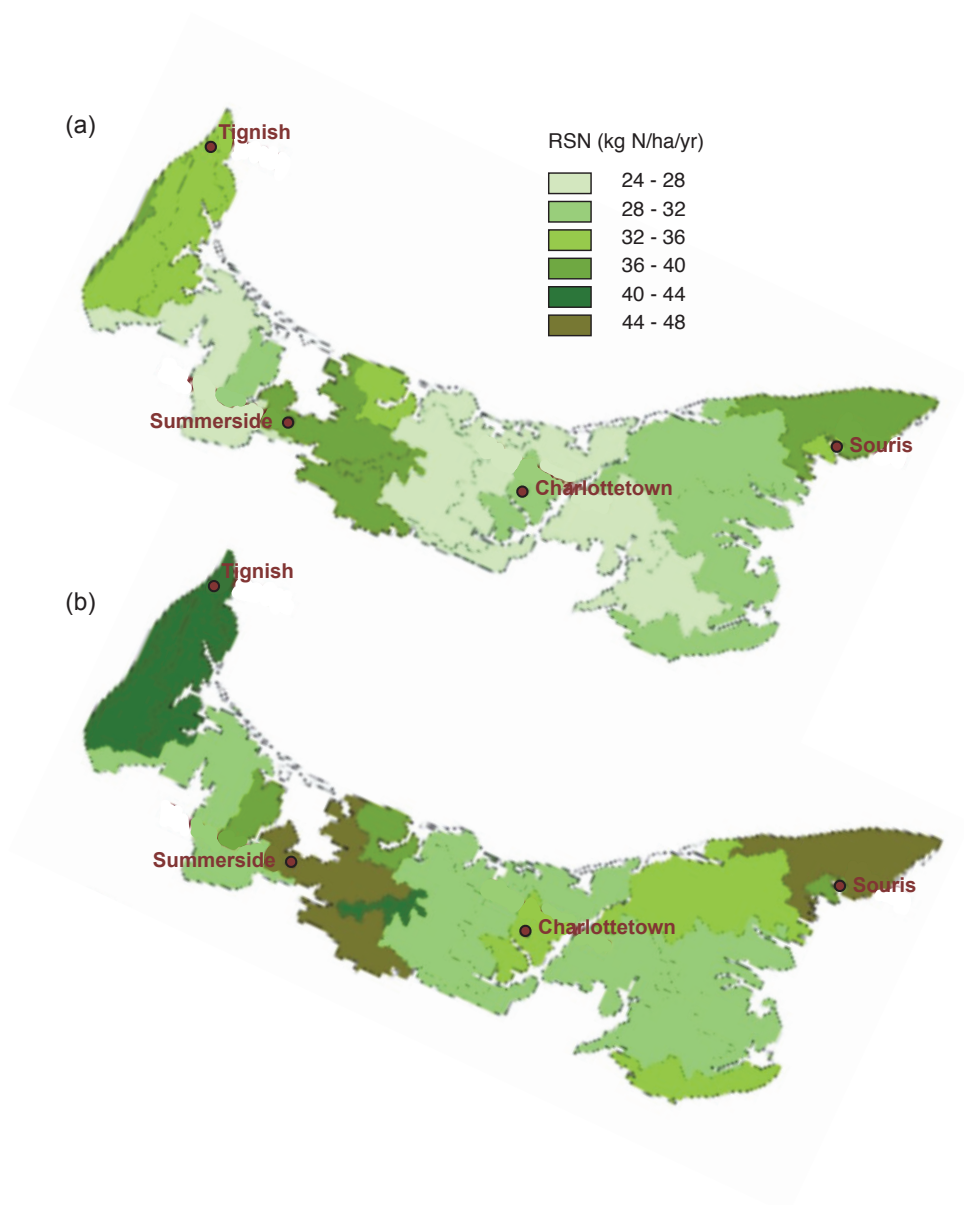
1064

1065



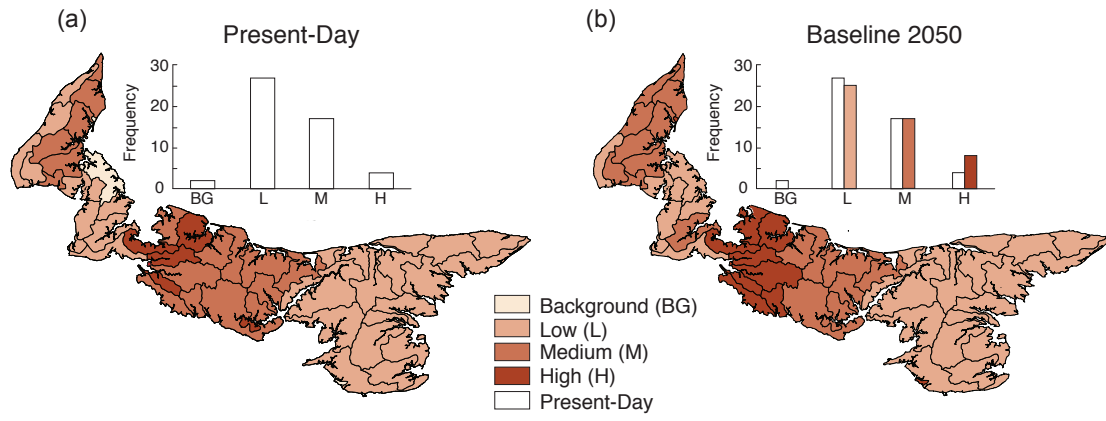
1066

1067



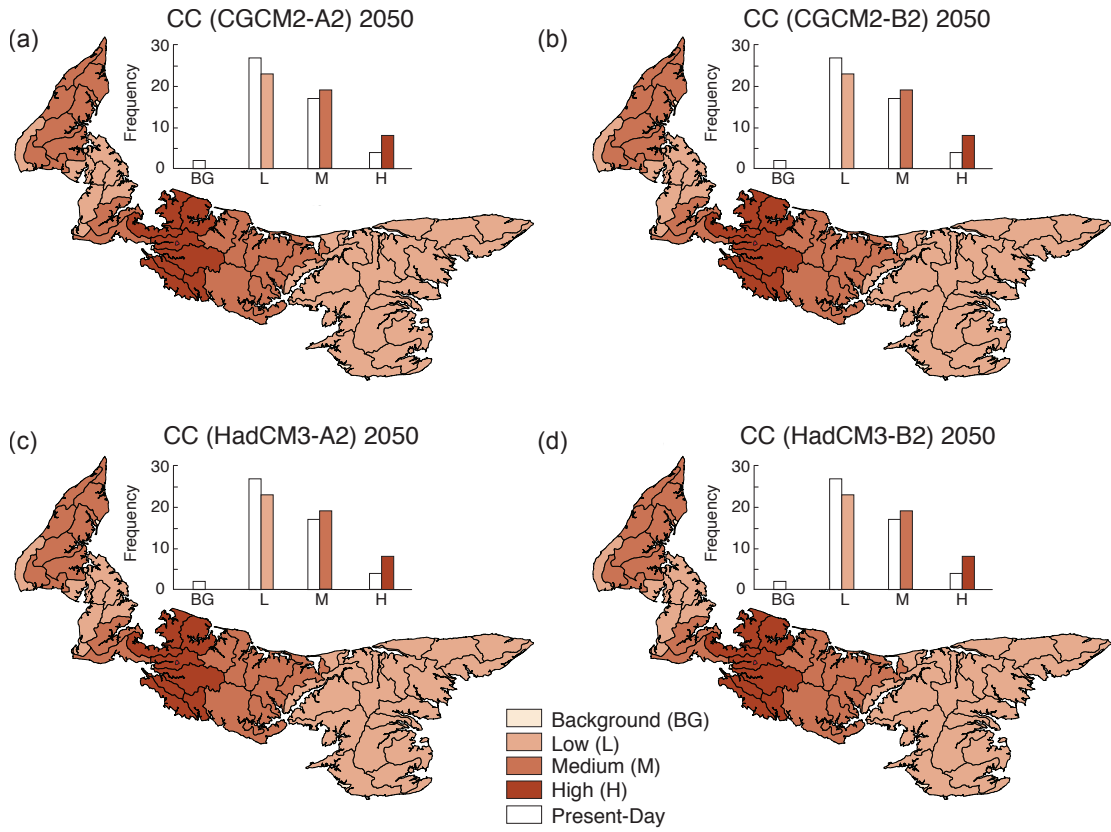
1068

1069



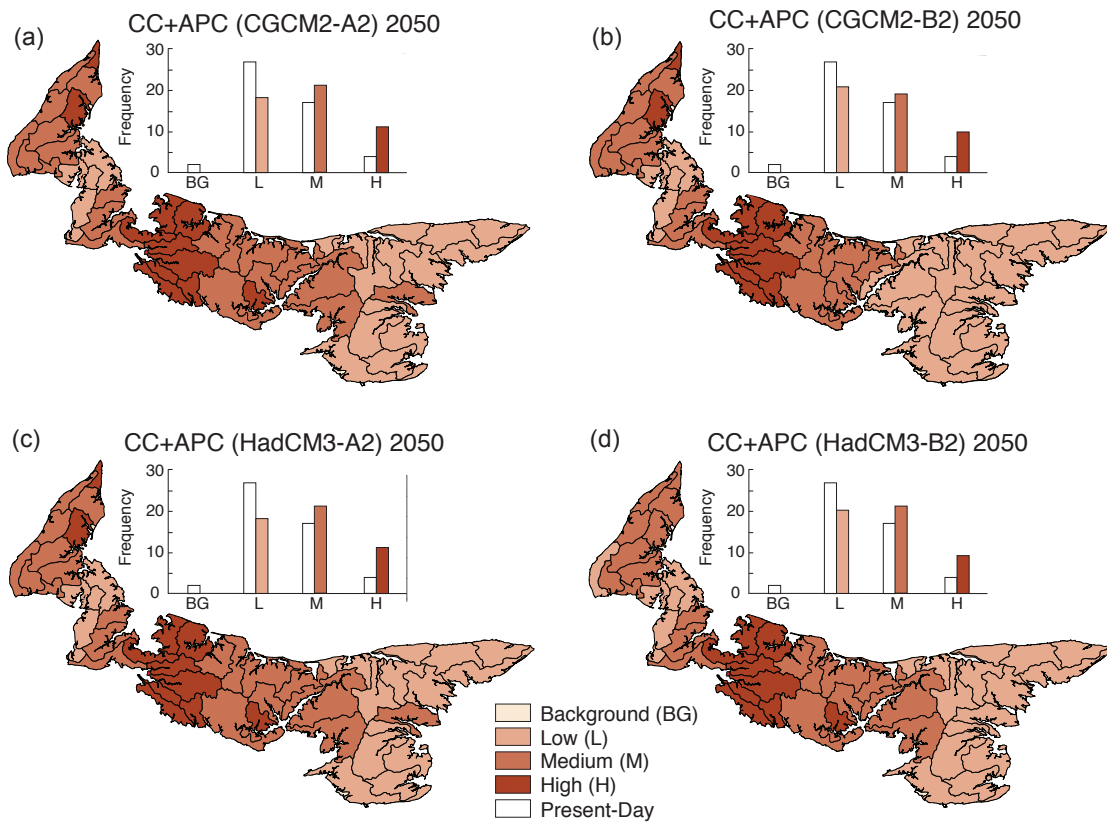
1070

1071



1072

1073



1074

1075

